

# REPORT DOCUMENTATION PAGE

*Form Approved*  
*OMB No. 0704-0188*

Public reporting burden for this collection of information is estimated to average 1 hour per response, including the time for reviewing instructions, searching existing data sources, gathering and maintaining the data needed, and completing and reviewing this collection of information. Send comments regarding this burden estimate or any other aspect of this collection of information, including suggestions for reducing this burden to Department of Defense, Washington Headquarters Services, Directorate for Information Operations and Reports (0704-0188), 1215 Jefferson Davis Highway, Suite 1204, Arlington, VA 22202-4302. Respondents should be aware that notwithstanding any other provision of law, no person shall be subject to any penalty for failing to comply with a collection of information if it does not display a currently valid OMB control number. **PLEASE DO NOT RETURN YOUR FORM TO THE ABOVE ADDRESS.**

<b>1. REPORT DATE (DD-MM-YYYY)</b> 03-Apr-2009		<b>2. REPORT TYPE</b> Technical Paper & Briefing Charts		<b>3. DATES COVERED (From - To)</b>	
<b>4. TITLE AND SUBTITLE</b>  <b>Experimental Characteristics of Particle Dynamics within Solid Rocket Motors Environments</b>				<b>5a. CONTRACT NUMBER</b> FA9300-08-M-3022	
				<b>5b. GRANT NUMBER</b>	
				<b>5c. PROGRAM ELEMENT NUMBER</b>	
<b>6. AUTHOR(S)</b> J.E. Moore & S.F. Son (Purdue University); Y.R. Sivathanu & J. Lim (En'Urga)				<b>5d. PROJECT NUMBER</b>	
				<b>5e. TASK NUMBER</b>	
				<b>5f. WORK UNIT NUMBER</b> 300508P3	
<b>7. PERFORMING ORGANIZATION NAME(S) AND ADDRESS(ES)</b>  En'Urga, Inc. 1291 Cumberland Avenue West Lafayette IN 47906				<b>8. PERFORMING ORGANIZATION REPORT NUMBER</b>  AFRL-RZ-ED-TP-2009-139	
<b>9. SPONSORING / MONITORING AGENCY NAME(S) AND ADDRESS(ES)</b>  Air Force Research Laboratory (AFMC) AFRL/RZS 5 Pollux Drive Edwards AFB CA 93524-7048				<b>10. SPONSOR/MONITOR'S ACRONYM(S)</b>	
				<b>11. SPONSOR/MONITOR'S NUMBER(S)</b> AFRL-RZ-ED-TP-2009-139	
<b>12. DISTRIBUTION / AVAILABILITY STATEMENT</b>  Approved for public release; distribution unlimited (PA #09154).					
<b>13. SUPPLEMENTARY NOTES</b> For presentation at the 56 <sup>th</sup> JANNAF Interagency Joint Propulsion Meeting, to be held in Las Vegas, NV, 14-17 April 2009.					
<b>14. ABSTRACT</b> Reliable measurements of the particulate dynamics and morphology within solid rocket motors are required to develop and validate numerical codes, as well as to develop improved understanding. For example, quantifying accurately the effect of binder systems on aluminum and alumina particle morphology in realistic environments is of great interest. An effort is underway to develop experimental methods to unobtrusively characterize the morphology and velocity of particles leaving the burning surface of a solid propellant. Atmospheric tests were considered first to develop and validate the diagnostic methods. Elevated pressure experiments were then conducted inside a windowed pressure vessel. Two composite propellants with different binders were considered, one consisting of HTPB/AP/Al and another with PBAN/AP/Al. The dynamics of aluminum and alumina particles formed during the combustion were accurately tracked, even on and near the propellant surface. A maximum velocity of ~7.21 ft/s (2.2 m/s) in the axial direction was observed during testing of the HTPB/AP/Al propellant, while a maximum velocity of 6.33 ft/s (1.93 m/s) was observed for the AP/PBAN/AL, both at 1 atm. The maximum velocity for the PBAN/AP/Al propellant decreased to 5.38 ft/s (1.64 m/s) during the elevated pressure tests. Distinct differences in the morphology of the particles, caused by the different binder systems used in the propellant mixtures, can be clearly seen in the results. During the experiments, images were gathered at 6000 frames per second by a high-speed camera using a variety of optics and filters. The gathered data was processed using statistical image correlation velocimetry. Results were also obtained in cross flow using a modified windowed motor.					
<b>15. SUBJECT TERMS</b>					
<b>16. SECURITY CLASSIFICATION OF:</b>			<b>17. LIMITATION OF ABSTRACT</b>	<b>18. NUMBER OF PAGES</b>	<b>19a. NAME OF RESPONSIBLE PERSON</b>
<b>a. REPORT</b>	<b>b. ABSTRACT</b>	<b>c. THIS PAGE</b>			Mr. Hieu Nguyen
Unclassified	Unclassified	Unclassified	SAR	51	<b>19b. TELEPHONE NUMBER</b> (include area code) N/A

# EXPERIMENTAL CHARACTERISTICS OF PARTICLE DYNAMICS WITHIN SOLID ROCKET MOTORS ENVIRONMENTS

J.E. Moore and S. F. Son  
Purdue University  
West Lafayette, IN

Y.R. Sivathanu and J. Lim  
En'Urga Inc.  
1291-A Cumberland Avenue  
West Lafayette, IN 47906

## ABSTRACT

Reliable measurements of the particulate dynamics and morphology within solid rocket motors are required to develop and validate numerical codes, as well as to develop improved understanding. For example, quantifying accurately the effect of binder systems on aluminum and alumina particle morphology in realistic environments is of great interest. An effort is underway to develop experimental methods to unobtrusively characterize the morphology and velocity of particles leaving the burning surface of a solid propellant. Atmospheric tests were considered first to develop and validate the diagnostic methods. Elevated pressure experiments were then conducted inside a windowed pressure vessel. Two composite propellants with different binders were considered, one consisting of HTPB/AP/Al and another with PBAN/AP/Al. The dynamics of aluminum and alumina particles formed during the combustion were accurately tracked, even on and near the propellant surface. A maximum velocity of  $\sim 7.21$  ft/s (2.2 m/s) in the axial direction was observed during testing of the HTPB/AP/Al propellant, while a maximum velocity of 6.33 ft/s (1.93 m/s) was observed for the AP/PBAN/AL, both at 1 atm. The maximum velocity for the PBAN/AP/Al propellant decreased to 5.38 ft/s (1.64 m/s) during the elevated pressure tests. Distinct differences in the morphology of the particles, caused by the different binder systems used in the propellant mixtures, can be clearly seen in the results. During the experiments, images were gathered at 6000 frames per second by a high-speed camera using a variety of optics and filters. The gathered data was processed using statistical image correlation velocimetry. Results were also obtained in cross flow using a modified windowed motor. The preliminary design of an entirely new windowed combustor has also begun so that these propellants can be studied in more detail at conditions similar to those in operating solid rocket motors.

## INTRODUCTION

The development of a robust system to diagnose particle dynamics is essential in the development of advanced propulsion systems. Many of these advanced propulsion systems are likely to include aluminized composite propellants. The addition of aluminum (Al) to a propellant improves its performance and can suppress high-frequency combustion instabilities [1]. During the combustion of aluminized composite propellants molten aluminum particles agglomerate on the burning surface.

Distribution A: Approved for public release; distribution unlimited

This research is sponsored by the Department of Air Force under the Small Business Innovative Research contract No. FA9300-08-M-3022. Special Thanks to Hieu Nguyen at the Air Force Research Laboratory for his advice and encouragement. Thanks to the grad students and staff at the Purdue University Energetic Materials Laboratory for their help and guidance.

## ALUMINUM AGGLOMERATION

An advantage to the use of metalized propellants is the increase in specific impulse versus non metalized propellants [2]. During the combustion process, fragments of the metal melt and agglomerate on the burning surface. In the case of Al, coagulation of these melted particles leads to agglomerates as large as 0.008 in. (200  $\mu\text{m}$ ) at 3 atm [8]. Because these particles continue to react and interact after leaving the burning surface, their size continually changes as they traverse the motor. Coalescence and fragmentation of the particles leads to continued evolution of the particles size. This size evolution inside the motor affects both the heat release (reaction rate) and particle damping. Therefore, predicting and understanding these dynamics is critically important. Figure 1 is a schematic of the composition and makeup of an agglomerated Al particle. Only the outer surface of the molten Al and Al vapor is combusted and as the combustion process occurs, it produces, among other products, aluminum oxide ( $\text{Al}_2\text{O}_3$ ). This oxide first forms a shell around the molten Al droplet until it melts or breaks apart. Al and  $\text{Al}_2\text{O}_3$  are insoluble, resulting in the formation of an "oxide lobe" that is coupled with the Al droplet.

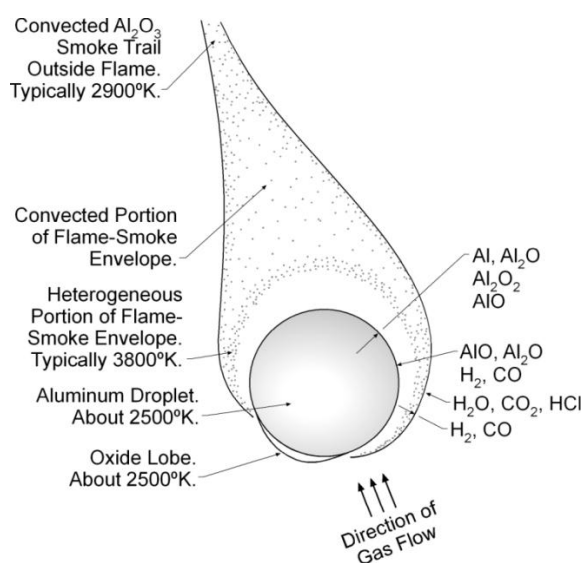


**Figure 1** Schematic of molten aluminum agglomerate droplet (adapted from [2]).

Many of the previous attempts to characterize these agglomerated Al particles have failed to adequately visualize particle formation on the burning surface and throughout the motor. Previous studies [3,11] have noted that in propellants which had bimodal distributions of ammonium perchlorate (AP) oxidizer, with the coarse distribution being much larger in diameter (typically 0.008 in. (200  $\mu\text{m}$ ) or more) than the fine, Al combustion occurs in the "pockets" formed by gaps in the coarse AP granules. At lower pressures, these "pockets" result in unfavorable ignition conditions and the formation of large agglomerates occur as partially combusted molten droplets combine. At higher pressures, more favorable ignition conditions are achieved, and the agglomeration size decreases. Hermsen [4] focused on the increase of particle size with respect to the throat diameter of the motor. Particles were collected from the exhaust via a quench method, and these particles were then empirically given a mass-weighted mean diameter. This particle size was found to increase exponentially with the throat diameter. Laredo [5] used a Malvern particle sizing instrument at the exit plane of the nozzle to gather the size of the particles. Another Malvern positioned in line with the combustion chamber just forward of the converging nozzle gave information about the nature of agglomerated particles near the subsonic region of the throat. The measurements yielded a multimodal distribution of particle sizes with a wide dynamic range. Averin [9] focused on the coagulation and fragmentation of particles in two phase flows due to sudden changes (both increasing and decreasing) in cross sectional area. The theoretical method developed showed that the mean diameter of aluminum oxide particles in an increasing-area duct could increase by a

factor of eight compared to their initial size. None of this previous work was able to accurately classify agglomeration near the burning surface of the propellant, and there was no velocity data gathered in the studies.

Kovalev [6] developed models to predict the agglomeration of Al on the burning surface as a function of propellant composition, pressure, burning rate, and size distribution of the AP oxidizer particles. This model was based on previous experimental results. Melcher [7] used a digital background subtraction/high-pass filter technique to measure the 2-D particle size of agglomerates. Using a chopper wheel and 35 mm camera, velocities of the larger (> 0.005 in. (120 μm)) agglomerated particles were obtained. These particle velocities were measured to be as high as 16.4 ft/s (5 m/s) at 13 atm.

## STATISTICAL IMAGE CORRELATION VELOCIMETRY

Statistical image correlation velocimetry is used to estimate the velocity field in the current experiment. The method works by assigning each pixel a coordinate (j). For each pixel, there is a light intensity,  $V_k^j$ , at time k. Equation (1) defines the cross correlation coefficient,  $S_{ij}$  between two pixels:

$$S_{ij} = \frac{\sum_{k=1}^N \left[ V_k^i(t) - \overline{V^i(t)} \right] \left[ V_k^j(t') - \overline{V^j(t')} \right]}{N \sqrt{\sigma_i(t) \cdot \sigma_j(t')}} \quad (1)$$

The time difference (t-t') is the lag between the images. N is the total numbers of pixels in the image. The variable  $\overline{V^i(t)}$  is the mean intensity obtained at pixel (i) at the specified time t from the ensemble of images, and  $\sigma_i(t)$  is the variance. Next, the velocity U(x,y,t) is estimated from the peak displacement of the intensity of each specific pixel. To obtain the peak displacement of the particular intensity, the entire field of pixels is searched for a pair of pixels (i,j) that provides the highest correlation coefficient. For the highest correlation pair, the displacement distance is divided by the time lag to give the mean velocity.

## EXPERIMENT

The system feasibility was evaluated using open atmosphere tests. Figure 2 shows an overhead schematic for the open atmosphere setup. The system had three major components: A Vision Research Phantom v 7.3 high speed camera in conjunction with a 105 mm Nikon Nikkor lens; a 100W Xenon Lamp; an aluminized propellant strand; a laptop equipped with Phantom camera control software. An image of the setup is shown in Fig. 3.

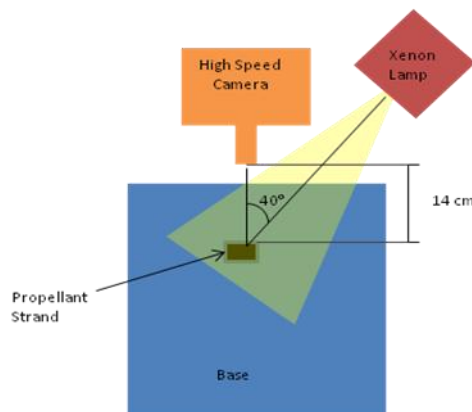


**Figure 2** Schematic of open atmosphere setup.

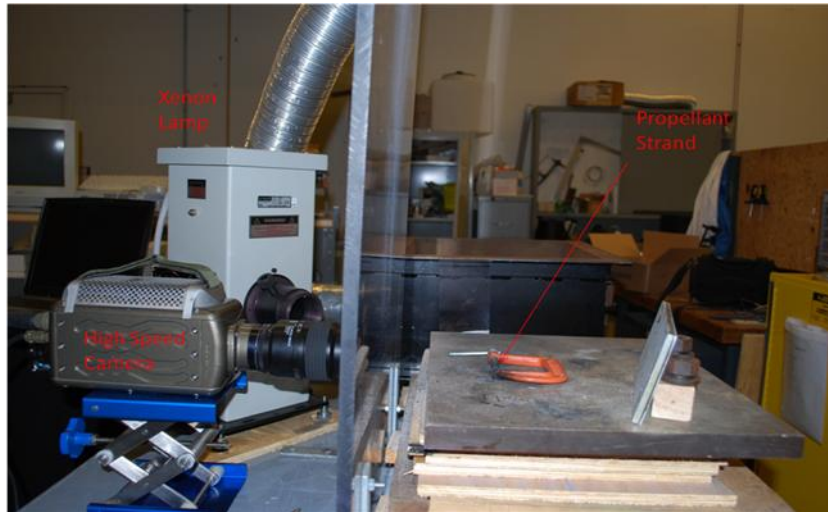


**Figure 3** Image of open atmosphere setup.

Open atmosphere testing allowed for quick adjustments to experimental parameters such as the camera-to-sample distance. Adjustments were made until the setup was optimized for obtaining the required data. Optimizing these parameters made the transition to testing inside of the pressure vessel, where changes to setup were more difficult, a much simpler process. A sequence of representative images is shown in Fig. 4.

Two different types of aluminized propellants were used during the study. The first was mixed with hydroxyl-terminated polybutadiene (HTPB) binder while the second utilized polybutadiene acrylonitrile (PBAN). Table 1 gives the binder/oxidizer/fuel formulations for the two propellants used in the experiments. The aluminum content, as a percentage of total mass, was the same for both propellants while the AP distributions and binder percentage differed some. The two binders produced very different agglomeration affects. Figure 5 shows a series of images gathered with the PBAN/AP/Al propellant. HTPB/AP/Al particles showed a tendency to agglomerate into small particles which would then form a chain before leaving the propellant surface. The PBAN/AP/Al particles would start in similar chains above the burning surface, but then agglomerate downward (toward the burning surface) into larger, more spherical particles before detaching from the surface. This downward motion is due to the effects of surface tension dominating the particles until they are overcome by aerodynamic forces causing the particle to detach from the surface [10].

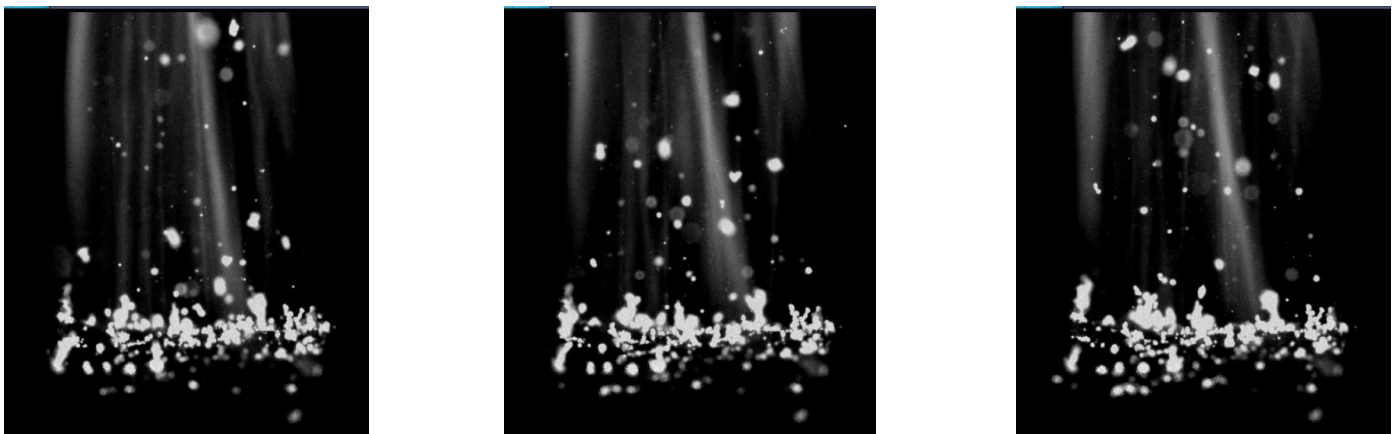


**Figure 4** Sequence of images for HTPB/AP/Al propellant. Time between images: (167  $\mu$ s).

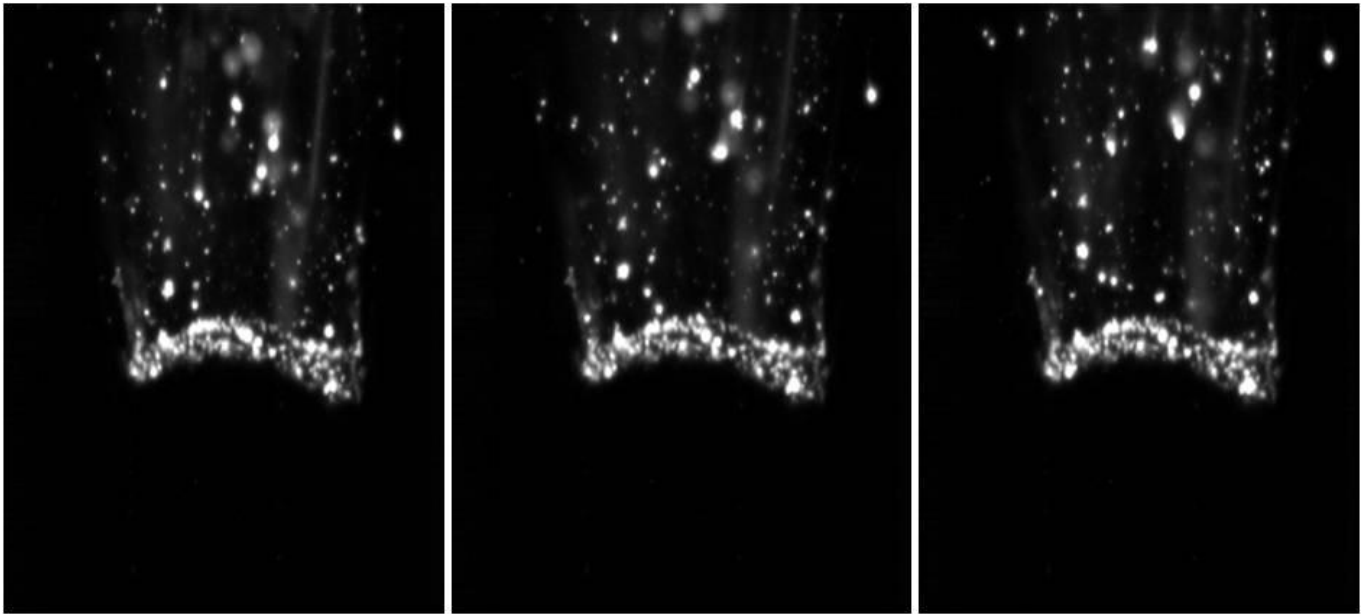


**Figure 5** Sequence of images for PBAN/AP/Al propellant. Time between images: (167  $\mu$ s).

**Table 1** Fuel/oxidizer/binder Combinations

Propellant	1	Wt. %	2	Wt. %
Fuel	AL (196 $\mu$ in. (5 $\mu$ m))	16	Al (472 $\mu$ in. (12 $\mu$ m))	16
Oxidizer	AP (.008 in. (200 $\mu$ m))	32.2	AP (.008 in. (200 $\mu$ m))	48.8
	AP (.002-.005 in. (60-130 $\mu$ m))	32.2	AP (.004 in. (90 $\mu$ m))	20.9
Binder	HTPB	15	PBAN	12

Inhibitors were employed to avoid flame spread down the side of the propellant samples. Two commercially available coatings were applied for this study. The first was a spray-on polyurethane, and the second was a clear enamel spray paint. Both inhibitors were applied via aerosol cans. During final preparation, a sample would be sprayed with up to three applications of a particular inhibitor. The samples were given anywhere from two to 10 minutes to cure between the applications. In most cases, the samples were allowed to cure for a minimum of 24 hours before the strand burns were initiated. There were a couple of experiments performed where the inhibitor curing time was less than six hours, but there was no recognizable difference in burn characteristics between the 6-hour and 24-hour cured samples. Of the two inhibitors considered, the clear enamel had the best results. Frequent side burning of polyurethane-inhibited strands made it less desirable for future testing, and it was discontinued. Figure 6 shows the strand holder and a typical sample. During the HTPB/AP/Al test, the distance from the camera to the sample was approximately 5.51 in. (14 cm). This ensured a very clear and crisp view of the propellant surface. During later tests, this distance was increased to 12.80 in. (32.5 cm) to maintain roughly the same field-of-view at lower resolutions. This was done to compensate for a decreased camera detector area at lower resolutions. The propellant strands were held secure in a clamp which actually led to the formation of some recirculation regions near the edges of the propellant. Ignition was achieved using a propane torch. At the instant of ignition, the camera triggered to begin capturing data.

Data was analyzed using SICV software developed by En'Urga, Inc. A scale image was taken prior to ignition of a sample. This scale was used to calculate an mm/pixel value for each sample. The mm/pixel value was vital in resolving the distance traveled by each particle. In order to ensure that no transients were used to calculate the steady-state velocity field, the first 100 frames of each dataset were not analyzed. A correlation coefficient plot for an HTPB/AP/Al sample is shown in Fig. 7. High values of the correlation coefficient validate the assumption that the video quality is sufficient for calculating the velocity field. Figure 8 shows axial and radial velocity field values obtained during the open atmosphere burns of the HTPB/AP/Al propellant. Axial

Velocities in the upper regions of the image frame (away from the burning surface) reached values of 7.21 ft/s (2.2 m/s). The radial velocities were very near zero for a majority of the images. There were some negative velocity regions near the sides of each image, and these were likely attributed to recirculation zones. The axial velocity of agglomerates of the PBAN/AP/Al was slightly less than what was calculated for the HTPB/AP/Al propellant. A correlation coefficient and pair of velocity field plots is shown in Fig. 9. The maximum axial velocity was calculated to be about 6.33 ft/s (1.93 m/s). The non-zero radial velocities are again attributed to the recirculation regions.

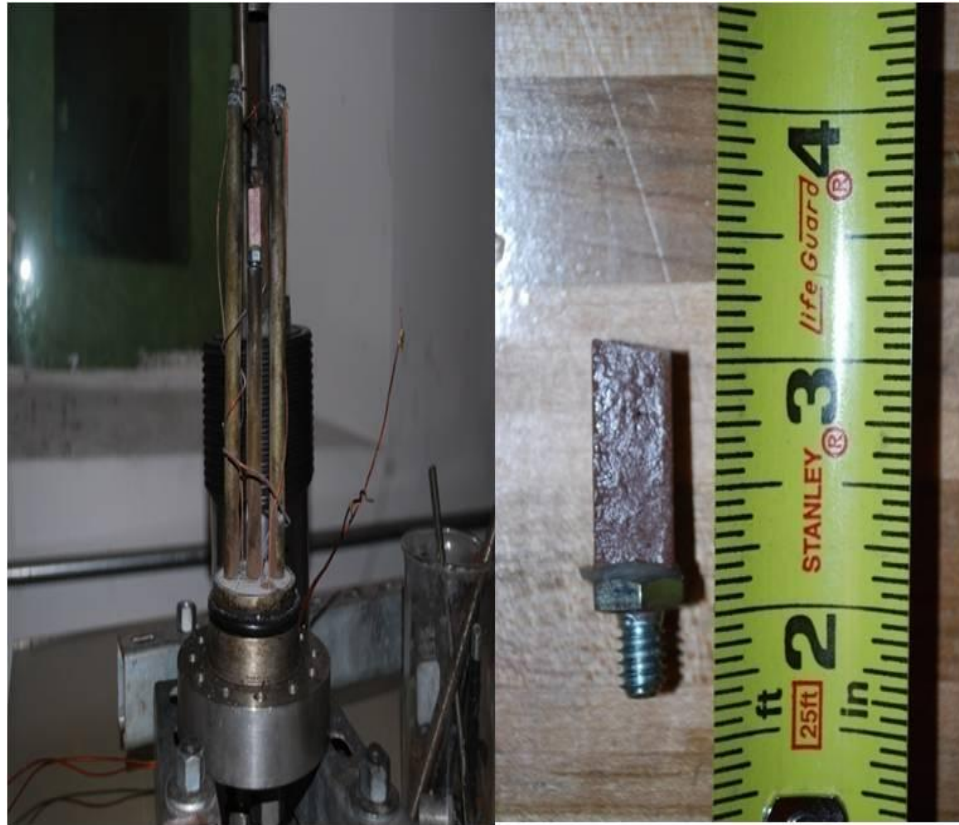


**Figure 6** Strand holder and inhibited propellant strand.

After validating the setup using open atmosphere tests, the experiments were reproduced inside of a pressure vessel rated to 1000 psi. Figure 10 shows the test setup inside of the bomb. Many of the components from the initial open atmosphere tests were used in this portion as well. One major addition was the use of a diffuser to evenly distribute the light from the Xenon Lamp. Because of the increased brightness of the burning strand at these higher pressures, the lamp was only used during the positioning of the strand and the focusing of the camera. Tests were conducted at 60 psig (~4 atm) via a pressurization system consisting of 99.99% argon gas. A nickel/chromium wire, coiled on the middle of the burning surface was used to supply the heat of ignition. At the instant of ignition, the camera was triggered. Argon gas was continuously circulated during the test to ensure that combustion exhaust products did not inhibit the view of the burning surface.

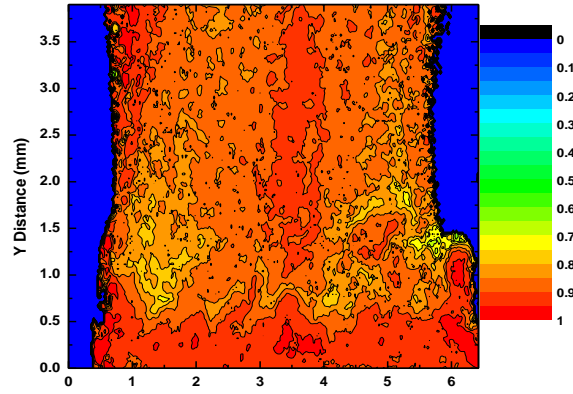


Figure 7 Correlation coefficient of an image set.

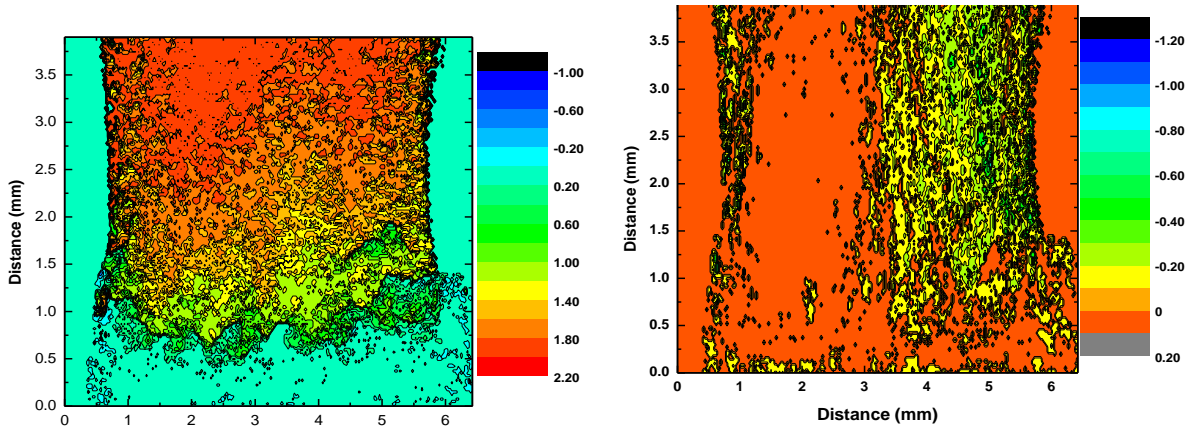


Figure 8 Sample axial & radial velocities.

The correlation coefficient and velocity fields for a PBAN/AP/Al test inside of the pressure vessel are shown in Fig. 10. The maximum velocity decreased to approximately 5.38 ft/s (1.64 m/s). A brief discussion of continuity supports this finding. Mass flow continuity for the combustion products can be expressed as,

$$\rho_c r_b A = \rho_g V A, \quad (2)$$

where  $\rho_c$  is the condensed phase propellant density,  $r_b$  is the propellant burning rate,  $\rho_g$  is the gas phase density of the propellant,  $V$  is the gas velocity, and  $A$  is the 2-D cross sectional area normal to the control volume in consideration. The propellant burning rate can be expressed using St. Robert's Law,

$$r_b = a P_g^n, \quad (3)$$

where  $a$  is the burning rate coefficient,  $P_g$  is the gas pressure and  $n$  is the burning rate exponent. Using the Ideal gas law, the gas density can be expressed as,

$$\rho_g = \frac{P_g}{RT_g}, \quad (4)$$

where  $R$  is the universal gas constant and  $T_g$  is the gas temperature (can be calculated using chemical equilibrium analysis). With these substitutions, the gas velocity can be expressed as,

$$V = C P_g^{n-1}, \quad (5)$$

where

$$C = a\rho_c RT_g. \quad (6)$$

Most propellants in use have a burn rate exponent less than 1, which leads to the conclusion that a pressure rise has the affect of decreasing gas velocity.

Spectral data was also gathered for the PBAN/AP/Al propellant at 4 atm, using a Spectraline Inc. ES-100 Mid-Infrared Spectrometer. Figure 12 shows the data. Peaks corresponding to light emission from the gas and gray body emission from the particles is evident. Future work will analyze these results further.

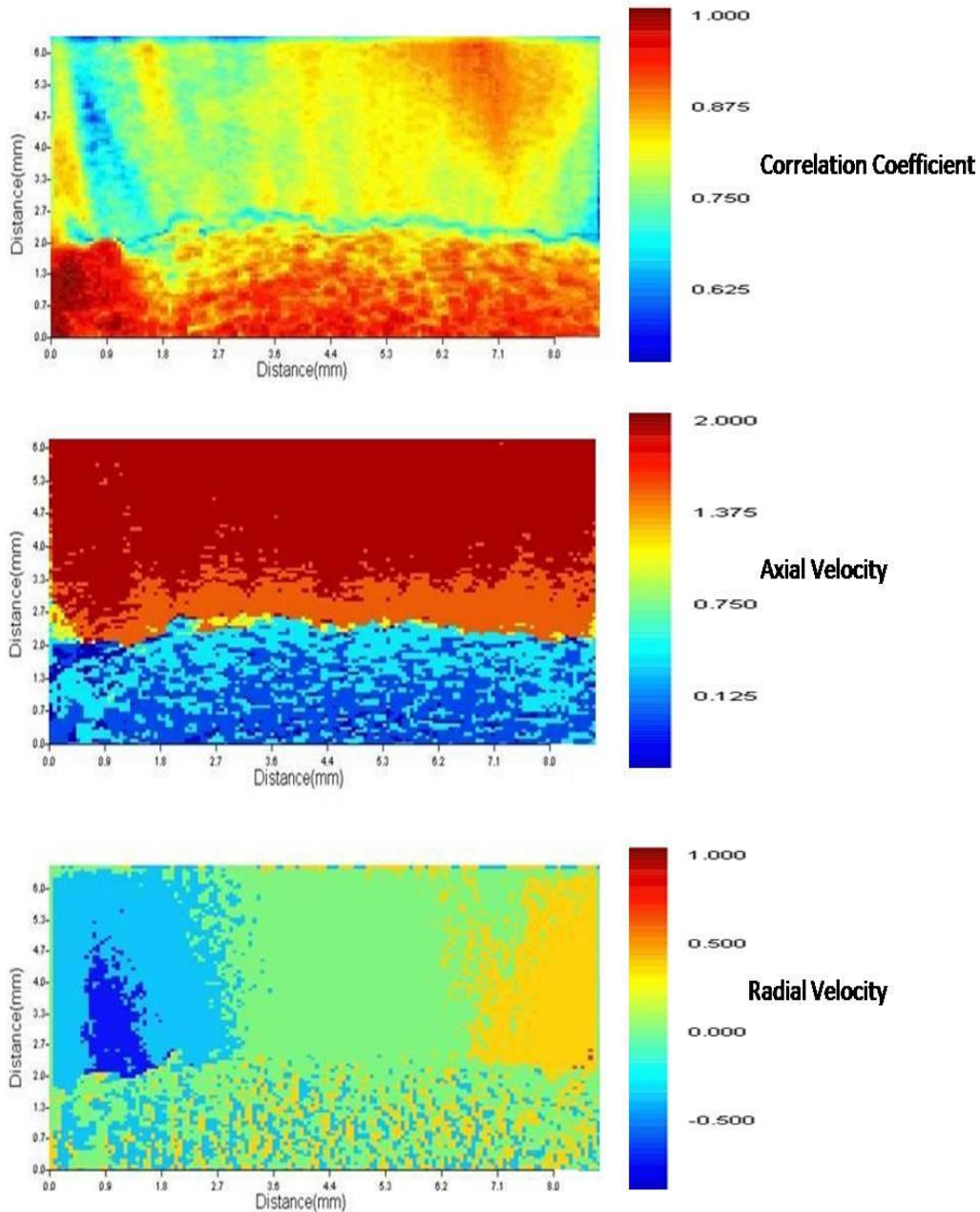


**Figure 9** Correlation coefficients and velocity fields for PBAN/AP/Al propellant at 1 atm.

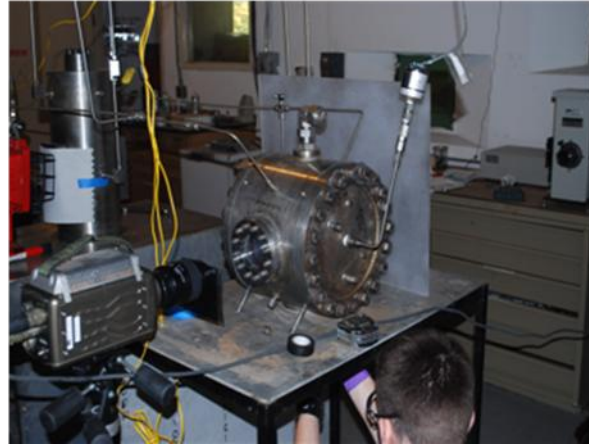
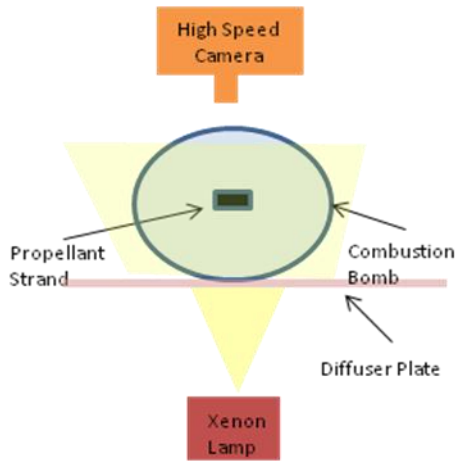


Figure 10 Pressure vessel experimental setup.

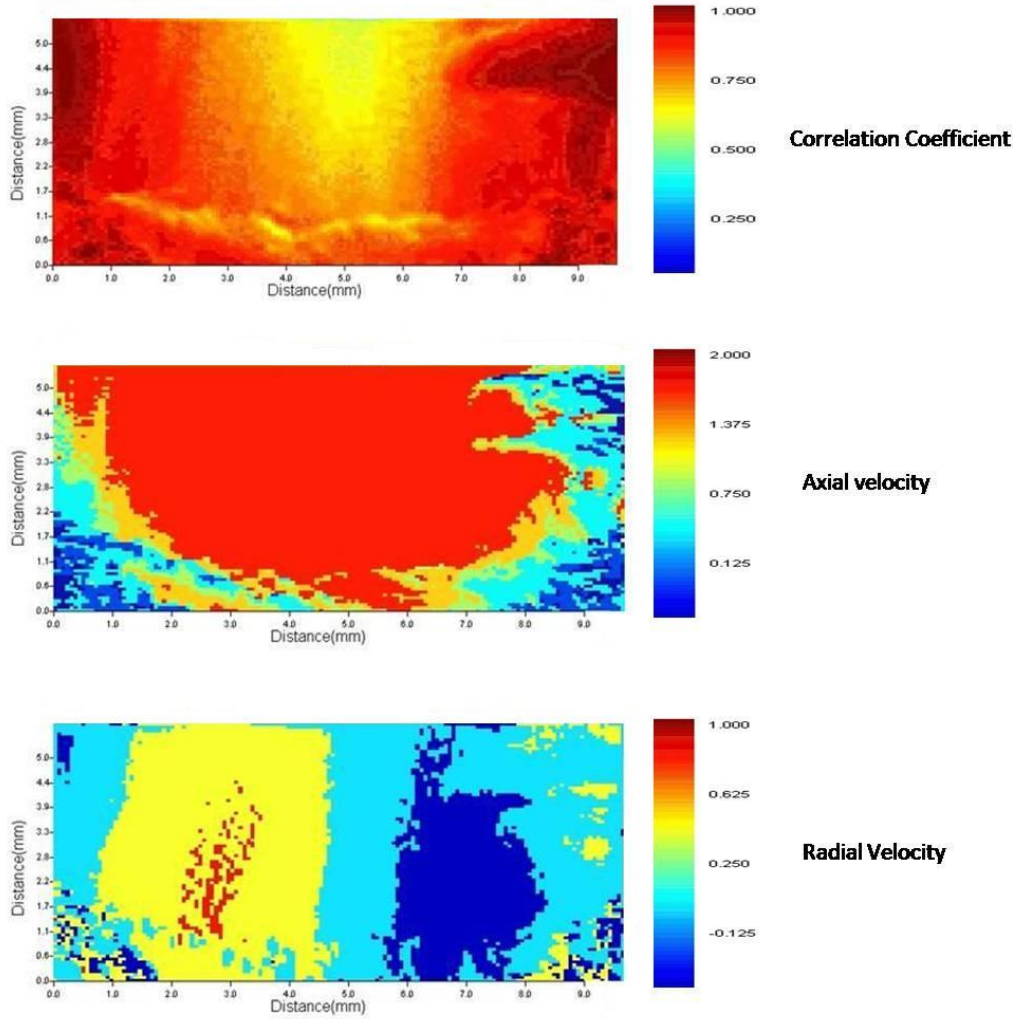
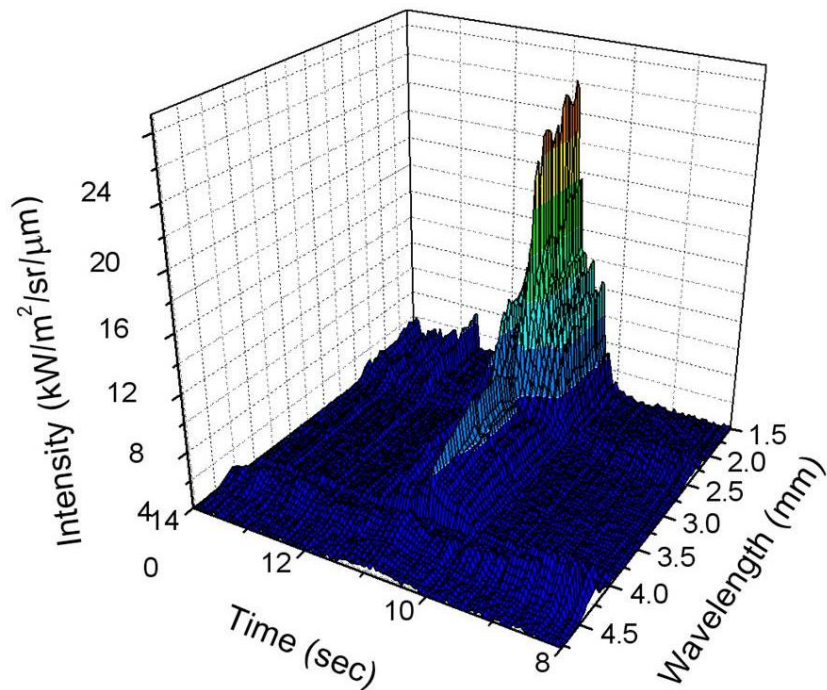
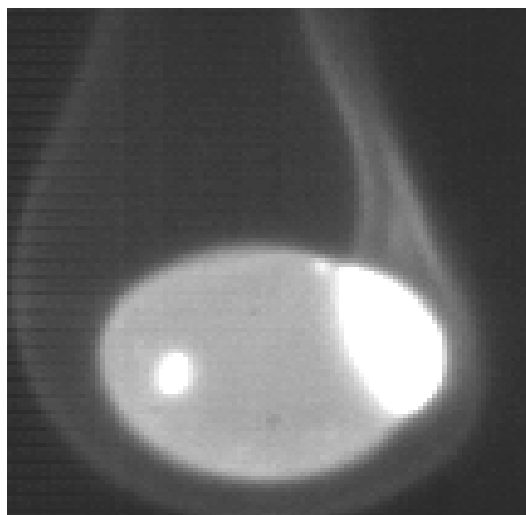


Figure 11 Correlation coefficient and velocity fields for PBAN/AP/Al propellant at 4 atm.



**Figure 12** Infrared spectrometer data gathered at 1 atm for propellant 1.

A microscopic imaging objective was used in conjunction with the high speed camera and lens to obtain a detailed view of the particle agglomeration. Figure 13 shows a microscopic view of an Al/Al<sub>2</sub>O<sub>3</sub> droplet. The bright oxide lobe is clearly visible on the right hand side of the figure. The droplet appears to be non-spherical. When formed at the surface, the agglomerations were virtually spherical, but some of these particles left the surface with a non-negligible rotational velocity. This rotational velocity coupled with the difference in liquid densities of Al and Al<sub>2</sub>O<sub>3</sub> caused some rotational deformation or “wobbling” of the particle as it traversed away from the burning surface. The non-spherical nature of the droplets makes velocity and particle size measurements more difficult as many sizing techniques assume a spherical particle in their calculations. The agglomeration phenomenon for the PBAN/Al/AP can clearly be seen in Fig. 14. The residence time this series of images was approximately 2.4 ms.



**Figure 13** Image of agglomerated aluminum droplet.

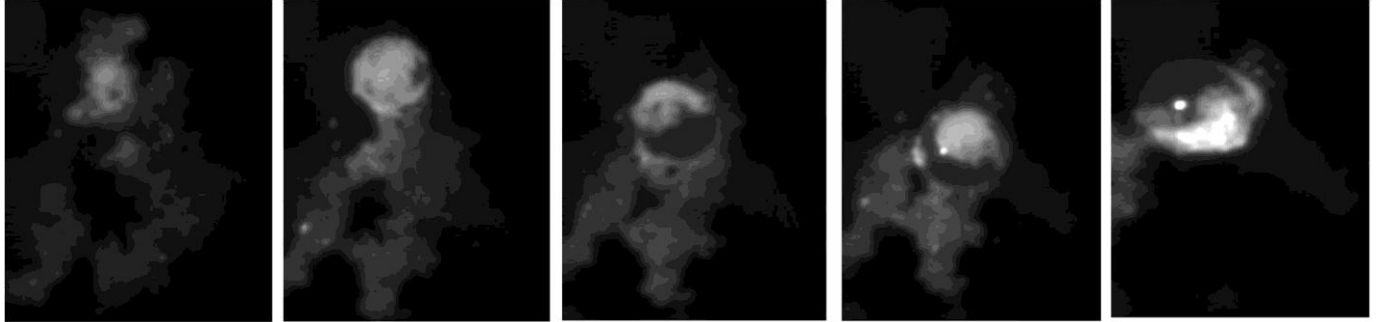


**Figure 14** Particle Agglomeration sequence. Residence time is 2.4 ms.

A particle diameter measurement tool, developed at Purdue University, was used to size agglomerates from a 1 atm burn of the PBAN/AP/Al propellant. The program measured the curvature of the boundary for a particular particle. It then searched the image for an equal and opposite curvature and the distance between these two curvatures was calculated to be the diameter. The program was originally designed to analyze images with multiple spherical particles per image, but was modified in order to accurately classify the non-spherical aluminum agglomerates. Typically only one particle would be in focus in a particular frame, so the confidence in the diameter measurements of the particles is very high. Figure 15 is a plot of the probability density function for the diameter measurements. The relative diameter on the x-axis (in mm) is the particle diameter multiplied by a factor of 16. The average particle size could be approximated by a Normal distribution with a mean of .011 in. (281  $\mu\text{m}$ ) with a standard deviation of .002 in. (51.2  $\mu\text{m}$ ) for a 95% confidence interval. This is an expected increase from the data reported in [8], due to the increased pressure. The data is based on 96 measurements taken on 13 distinct particles identified during the burn.

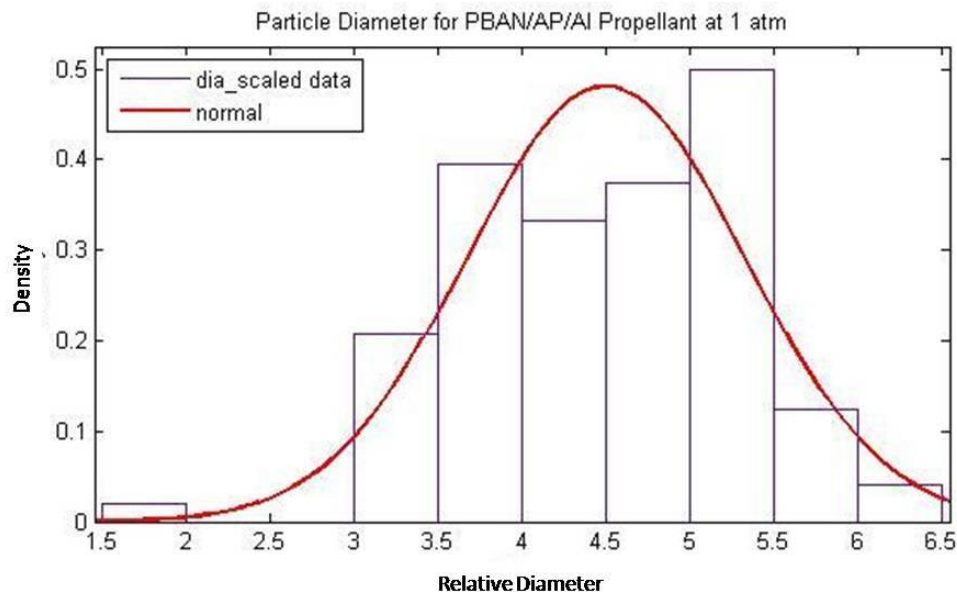


**Figure 15** Probability density curve for PBAN/AP/Al propellant at 1 atm.

In order to test proof-of-concept for future cross-flow studies, data was collected using an existing combustor currently optimized for the study of erosive burning. Figure 16 shows the windowed

combustor used. A propellant sample was placed in the proximity of the window, and ignited with a nickel/chromimium wire. In order to simulate the cross flow, nitrogen purge gases were flowed through the combustor. Figure 17 is a high speed still image taken during the test. The frame rate was again 6000 frames per second. Larger propellant samples were used in the hopes that more particle agglomeration and coalescence would be visible. The test proved successful in generating a cross flow, and agglomerates can clearly be seen traversing toward the aft end of the combustor.

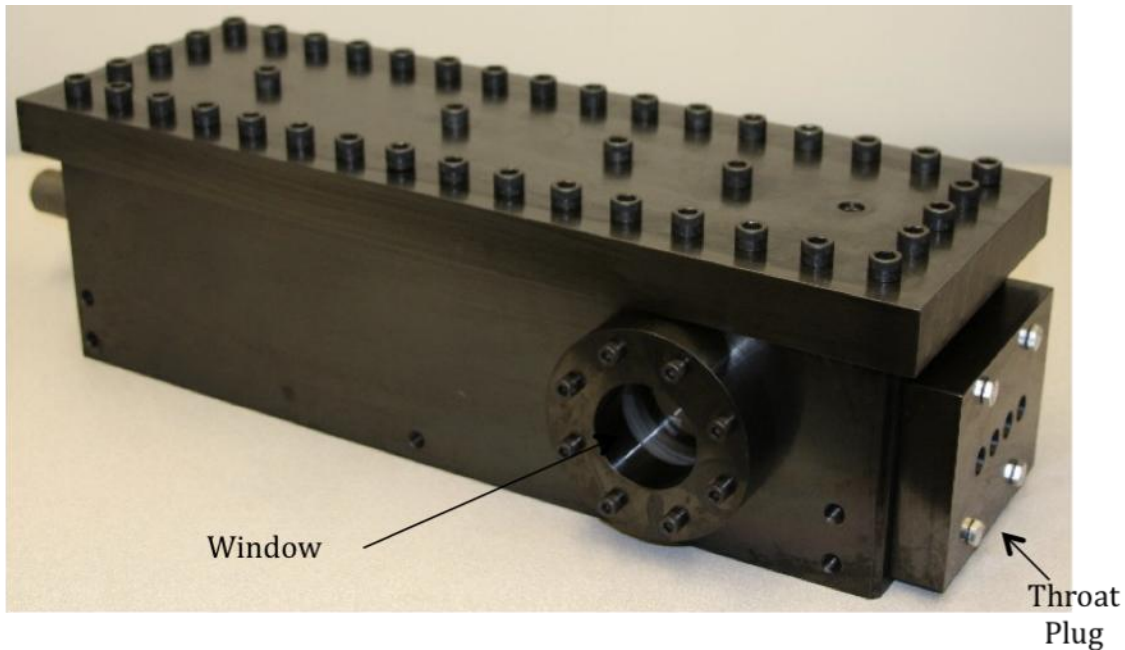


**Figure 16** Windowed combustor image.



**Figure 17** Agglomeration in cross flow.

### **SUMMARY AND CONCLUSIONS**

The experimental approach has proven to be viable in both open atmosphere tests as well as pressure vessel tests. The system allows for very easy transition between the two, and this will be utilized in future phases of the project to compare different fuel/oxidizer/binder combinations. Major conclusions from the current research are:

1. The agglomeration process for HTPB/AP/Al propellants is very different from that of PBAN/AP/Al propellants resulting in different particle shapes and velocities for the two types of propellants. These experimental observations resemble the processes described by [2]. Formulations differing only in binder composition will be mixed to further study this phenomenon.
2. The imaging system provides data that yields high values for the correlation coefficient. This indicates that the quality of the images produced by the imaging system is sufficient for measurements of the velocity field.
3. Particle velocity and size is dependent on gas pressure. Increasing the pressure yields larger agglomerates, but these agglomerates are moving at slower speeds due to a decreased gas velocity. This is supported by continuity analysis.
4. The diameter distribution of the agglomerates obeys a normal distribution. The particles change diameter as they traverse away from the burning surface, and they become non-spherical due to non-negligible rotational velocities. More analysis will be gathered to converge on an exact particle distribution, if applicable.

The results of the testing were found to be very repeatable. Three samples taken for the PBAN/AP/Al propellant yielded very similar results for the maximum axial velocity, and the velocity field data was comparable. Continued refining of the testing apparatus should improve on the results gathered here.

## FUTURE WORK

Work in the next phase will center on a windowed combustor which is currently in the preliminary design phase. This work will leverage technology already available at the university. The major modifications of the combustor will be the redesign of the window which will be elongated and positioned near the center of the combustor. Throat plug will have to be modified to ensure that the flow is choked when exiting the nozzle. Additional tasks to be completed include: Further velocimeter development and validation, velocity mapping in the solid rocket motor (SRM), particulate size development and validation, particulate characterization inside of SRM, and temperature inside of the SRM. The mixing capabilities at Purdue University will also be utilized to develop a variety of binder/oxidizer/fuel formulations to further study the affects of the different binders.

## REFERENCES

1. Cheung, H., Cohen, N. S., "Performance of Solid Propellants containing metal Additives," *AIAA Journal* 3(2), 250-257 (1964).
2. Price, E. W., "Combustion of Metalized Propellants," Chap. 9 in *Fundamentals of Solid-Propellant Combustion*, Kuo, K. K. and Summerfield, M (eds.), American Institute of Aeronautics and Astronautics, Inc., New York, pp 479-513 (1984).
3. Sambamurthi, J. K., Price, E.W., and Sigman, R. K., "Aluminum Agglomeration in Solid-Propellant Combustion," *AIAA Journal* 22(8), 1132-1138 (1984).
4. Hermsen, R. W., "Aluminum Oxide Particle Size for Solid Rocket Motor Performance Prediction, Proc. AIAA 19<sup>th</sup> Aerospace Sciences Meeting, Louis Missouri (January 1981).

5. Laredo, D., McCrorie, J. D., Vaughn, J. K., Netzer, D. W., "Motor and Plume Particle Size Measurements in Solid Propellant Micromotors," *Journal of Propulsion and Power* 10(3), 410-418 (1994).
6. Kovalev, O. B., "Motor and Plume Particle Size Prediction in Solid-Propellant Rocket Motors," *Journal of Propulsion and Power* 18(6), 1199-1210 (2002).
7. Melcher, J. C., Burton, R. L., Krier, H., "Combustion of Aluminum Particles in Solid Rocket Motor Flows," Proc. 35<sup>th</sup> AIAA/ASME/SAE/ASEE Joint Propulsion Conference and Exhibit, Los Angeles, CA (June 1999).
8. Mullen, J. C., Brewster, M. Q., "Characterization of Aluminum at the Surface of Fine-AP/HTPB Composite Propellants," Proc. 44<sup>th</sup> AIAA/ASME/SAE/ASEE Joint Propulsion Conference and Exhibit, Hartford, CT (July 2008).
9. Averin, V. S., Arkhipov, V. A., Vasenin, I. M., Dyachenko, N. N., Trofimov, V. F., "Effect of a Sudden Change in Cross-Sectional Area of the Solid Rocket Motor Duct on Coagulation of Condensed Particles," *Combustion, Explosion and Shock Waves* 39(3), 316-322 (2003).
10. Jackson, T. L., Najjar, F., Buckmaster, J., "New Aluminum Agglomeration Models and Their Use in Solid-Propellant Rocket Simulations," *Journal of Propulsion and Power* 21(5), 926-936 (2005).
11. Cohen, N. S., "A Pocket Model for Aluminum Agglomeration in Composite Propellants," Proc. 17<sup>th</sup> AIAA/SAE/ASME Joint Propulsion Conference, Colorado Spring, CO (July 1981).

# Experimental Characterization of Particle Dynamics within Solid Rocket Motors

By  
Joseph Moore  
&  
Steve F. Son, Ph.D.  
Purdue University

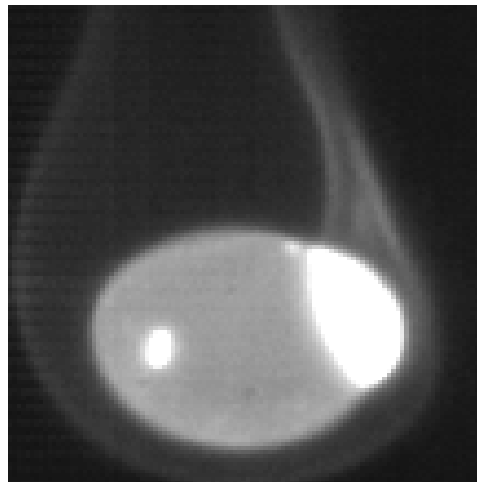
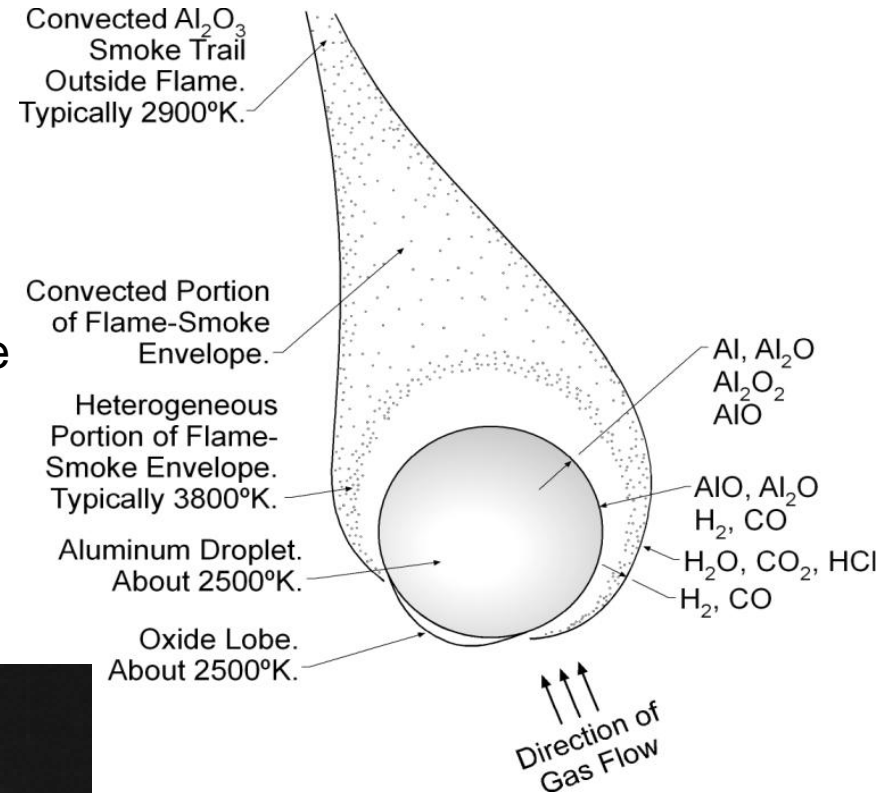
Yudaya Sivanathu, Ph.D.  
&  
Jongmook Lim, Ph.D.  
En'Urga Laboratories

Distribution A: Approved for public release; distribution unlimited

This research is sponsored by the Department of Air Force AFFTC/PKTB under the Small Business Innovative Research contract No. FA9300-08-M-3022.

# UNDERSTANDING OF THE PROBLEM

- Advantages to Aluminized propellants
  - Increase in specific impulse
  - Can suppress combustion instabilities
- Incomplete combustion of Al
  - Unfavorable ignition conditions on surface
  - Agglomerate into larger particles
  - Efficiency losses in system leads to decreased Isp from ideal



# PREVIOUS RESEARCH

- Price
  - Aluminum droplet model
  - Chain agglomeration for HTPB/AP/Al propellant
- Cohen
  - “Pocket Model”
  - Bi-modal AP distribution
  - Agglomeration between large particles
- Sambamurthi
  - Expanded on Pocket Model
  - Found that unfavorable ignition conditions in pockets led to large agglomerates
  - Certain conditions lead to the formation of “superagglomerates”
- Hermsen
  - Particle size v. throat diameter
- Averin
  - Effect of sudden changes in area
  - Size increase by factor of 8 from initial measurements

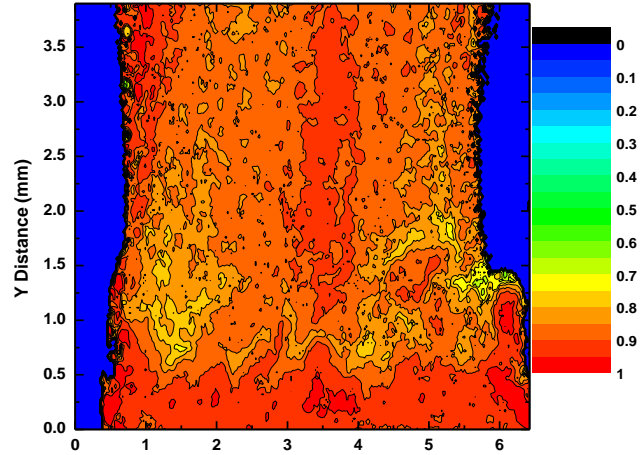
# PREVIOUS RESEARCH (CONT.)

- Kovalev
  - Agglomeration size v. composition, P, rb, AP size distribution
  - Based on experimental results
- Melcher
  - Digital background subtraction/high-pass filter
  - 16.4 ft/s (5 m/s) agglomeration size at 13 atm
- Mullen
  - Agglomerate size v. fine AP loading
  - 0.008 in. (200 micron) agglomerates at 3 atm
- Averin
  - Particle size based on sudden change (both increase and decrease) in motor area
  - Focused on both coagulation and fragmentation of particles

# OBJECTIVES

- Develop a statistical correlation velocimeter for obtaining high speed videos within a solid rocket motor
- Develop a high resolution imaging system to directly image particulates near the burn surface of a solid propellant inside a rocket motor
- Evaluate the two systems using a segment solid rocket motor

# STATISTICAL IMAGE CORRELATION VELOCIMETRY



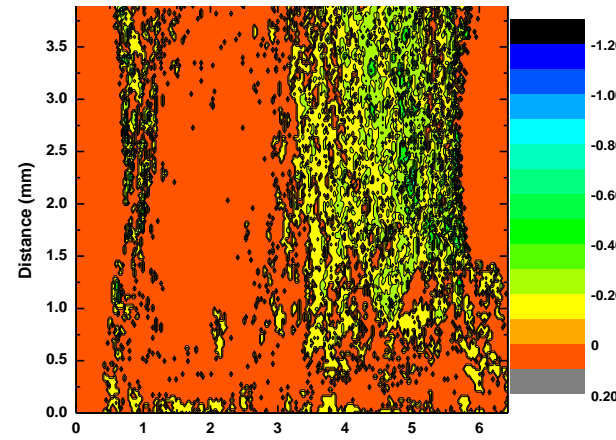
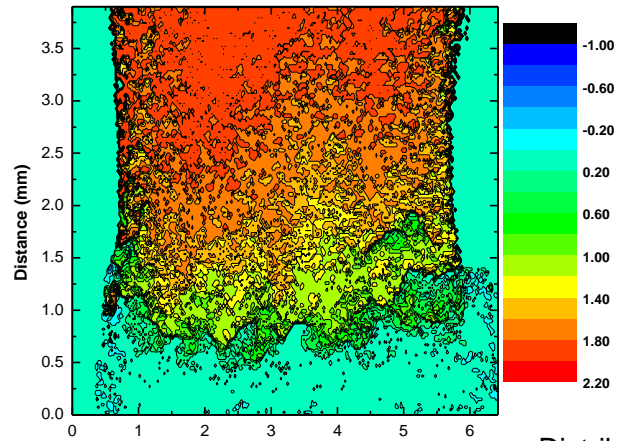
$$S_{ij} = \frac{\sum_{k=1}^N \left| \overline{V_k^i(t) - V^i(t)} \right| * \left| \overline{V_k^j(t') - V^j(t')} \right|}{N \sqrt{\sigma_i(t) \cdot \sigma_j(t')}}$$

•Inputs:

- High speed images
- Scale

•Outputs:

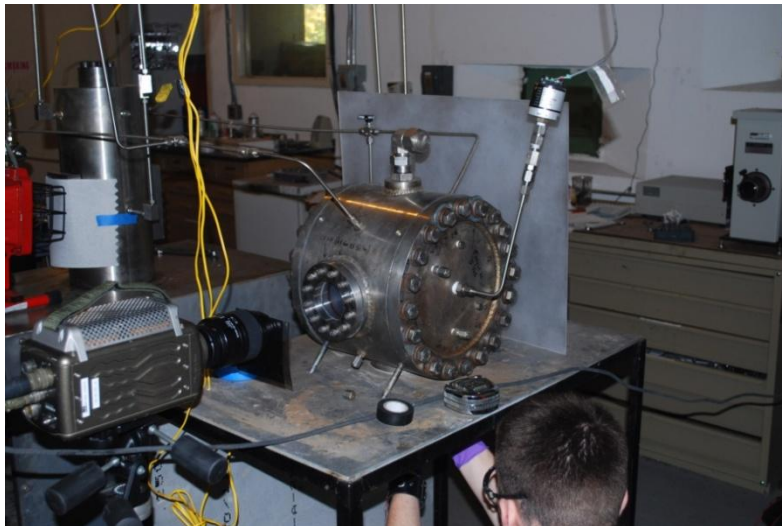
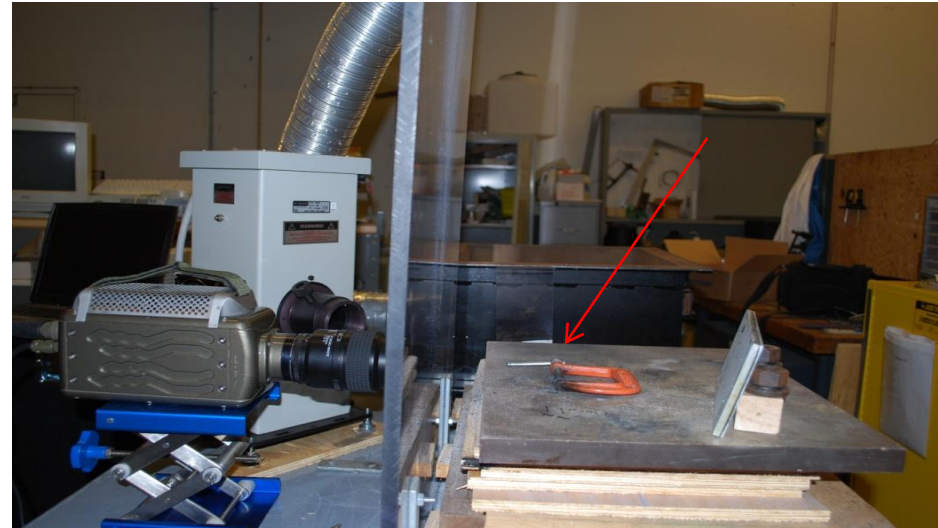
- Axial velocity
- Radial velocity
- Correlation coefficient



Distribution A: Approved for public release;  
 distribution unlimited

# IMAGING SYSTEM

- Phantom High Speed Camera
  - 6000 fps
  - 512x512 resolution
  - Later decreased to 256x256
  - 1-3  $\mu$ s exposure time
- 1000W Xenon Lamp
- ~5 second burn time



- 4 atm testing inside of pressure vessel
- Argon gas used for pressurization

Distribution A: Approved for public release;  
distribution unlimited

# AGGLOMERATION BASED ON BINDER



## HTPB/AP/Al propellants

- Flakes of Aluminum agglomerate into small particles which chain together before detaching from the burning surface

•Time between images: 167  $\mu$ s

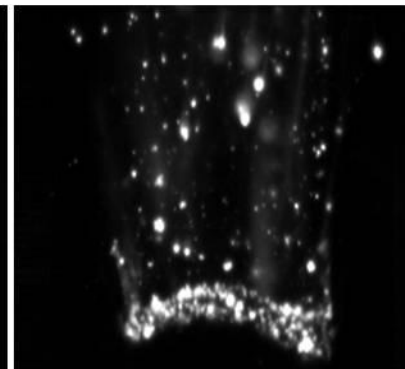
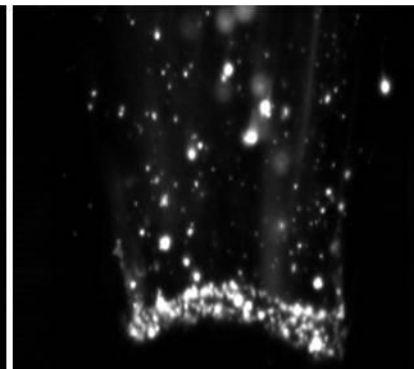
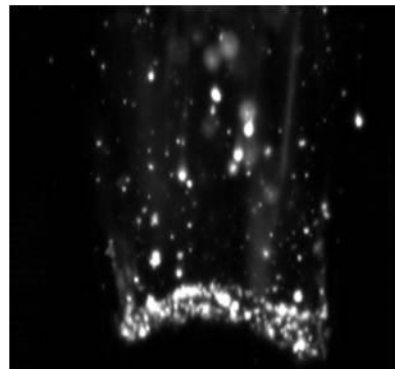
## PBAN/AP/Al Propellant

- Flakes of aluminum agglomerate downward toward surface into spherical particles

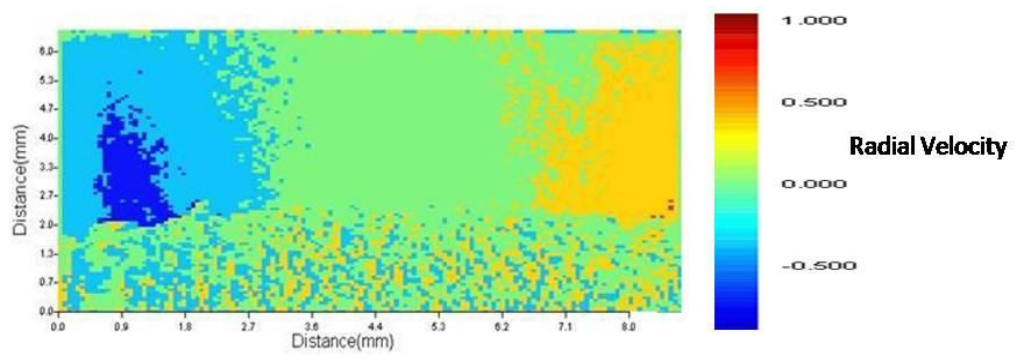
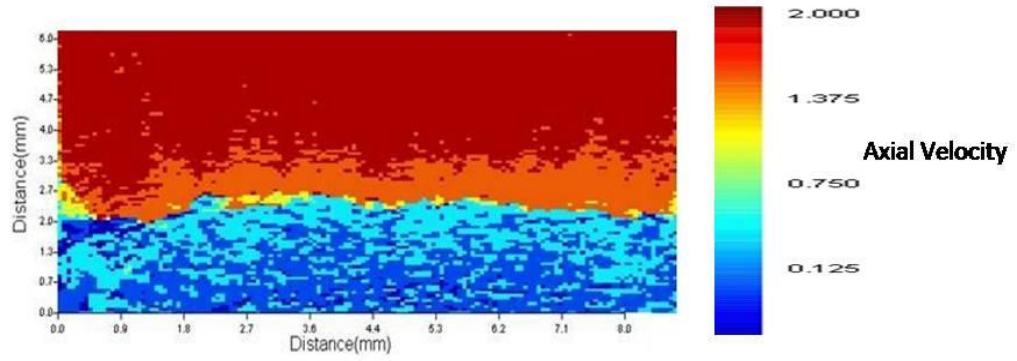
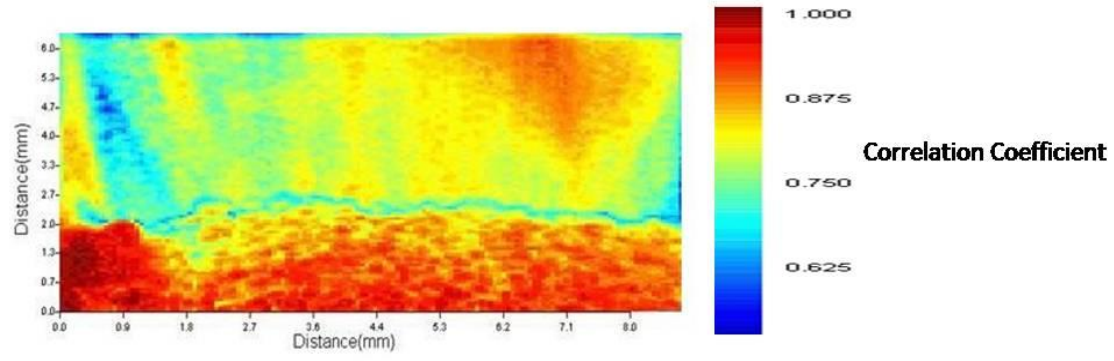
•Time between images:

167  $\mu$ s

Distribution A: Approved for public release;  
distribution unlimited



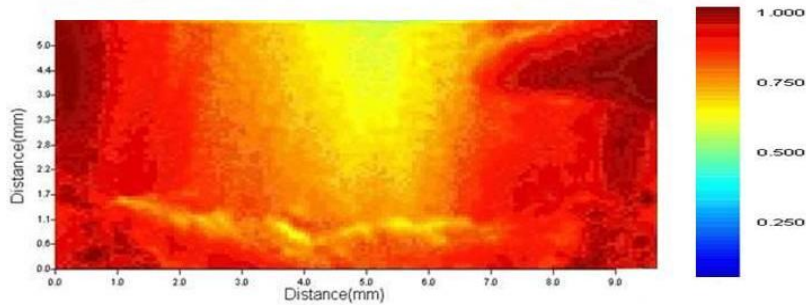
# PBAN/AP/AL AT 1 ATM



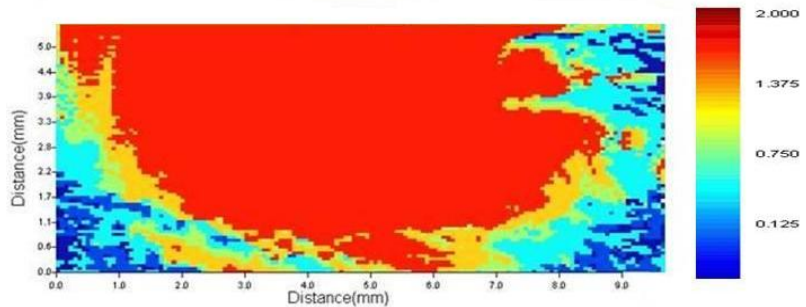
- High values for correlation coefficient
- Maximum velocity of  $\sim 6.33$  ft/s (1.93 m/s)
- Recirculation zones near edges of propellant due to clamping device

Distribution A: Approved for public release; distribution unlimited

# PBAN/AP/AL PROPELLANT AT 4 ATM

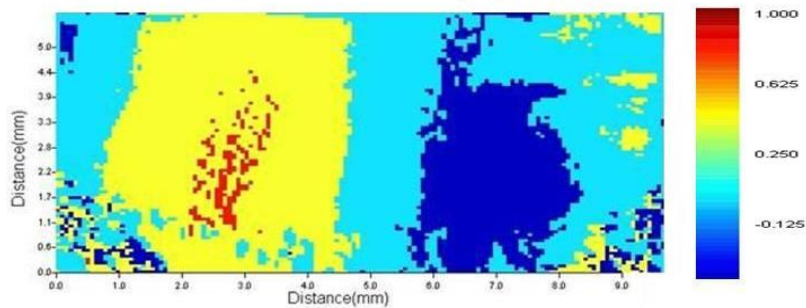


- High values for correlation coefficient



- Decreased maximum velocity  
~5.38 ft/s (1.64 m/s)

- Decrease in velocity validated by a discussion of continuity



Distribution A: Approved for public release;  
distribution unlimited

# DISCUSSION OF CONTINUITY

- Mass continuity for control volume is

$$\rho_c r_b A = \rho_g VA$$

- Burning rate (St. Roberts Law)

$$r_b = aP_c^n$$

- Ideal gas equation

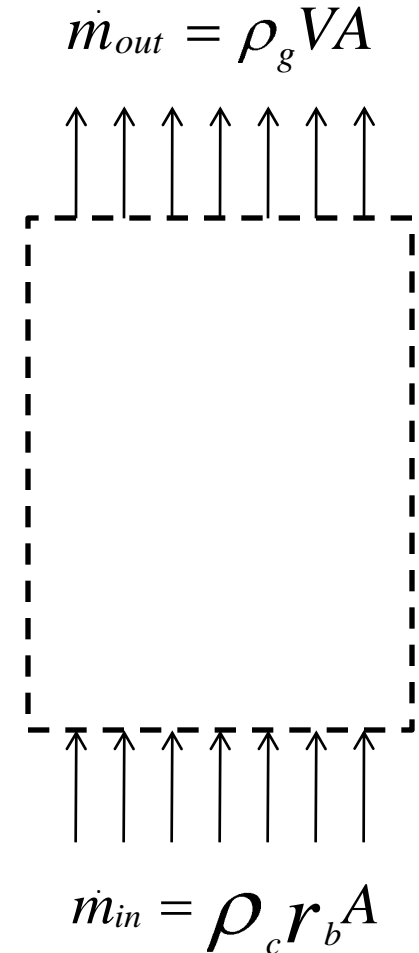
$$\rho_g = \frac{P_g}{RT_g}$$

- Combining to get velocity dependency

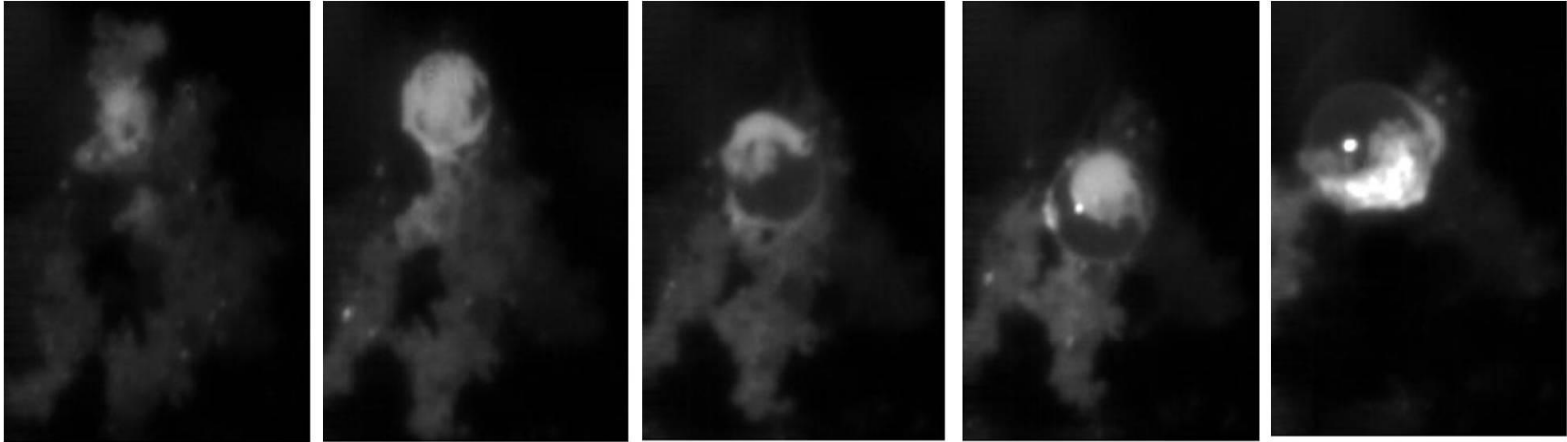
$$V = CP_g^{n-1}$$

$$C = a\rho_c RT_g$$

- Velocity is inversely proportional to Pressure



# MICROSCOPIC IMAGING

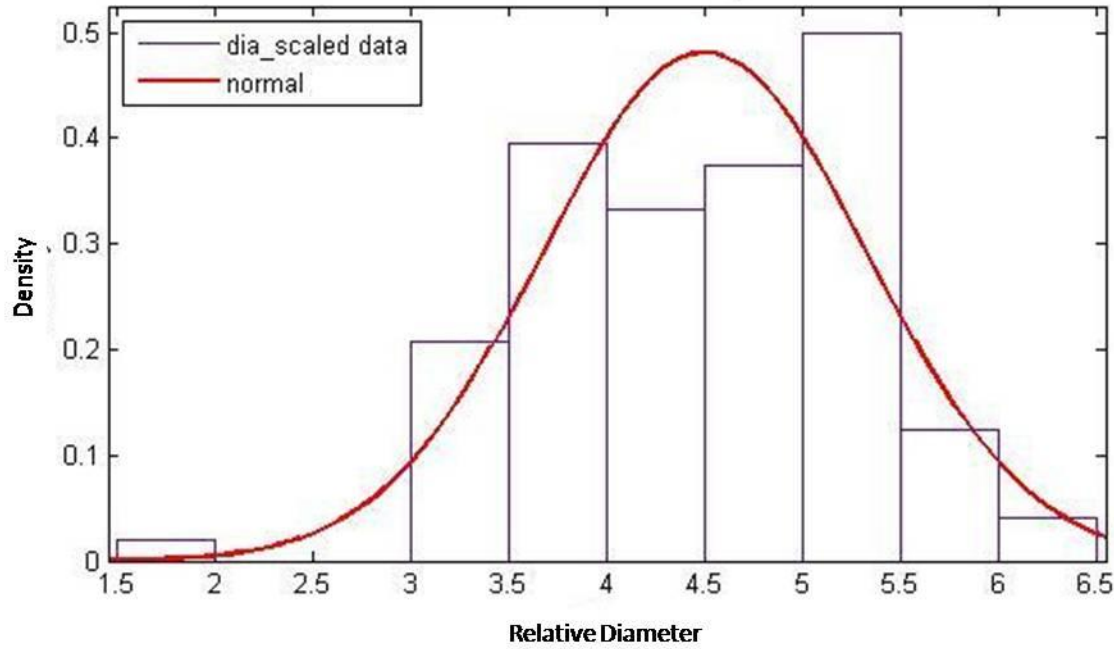


- PBAN/AP/Al Agglomerate at 1 atm
- Surface Tension drives particle toward burning surface until it is overcome by Aerodynamic forces
- Time  $\sim 2.4$  ms for above sequence
- Images analysis can be automated for particle sizing

Distribution A: Approved for public release;  
distribution unlimited

# PARTICLE SIZING

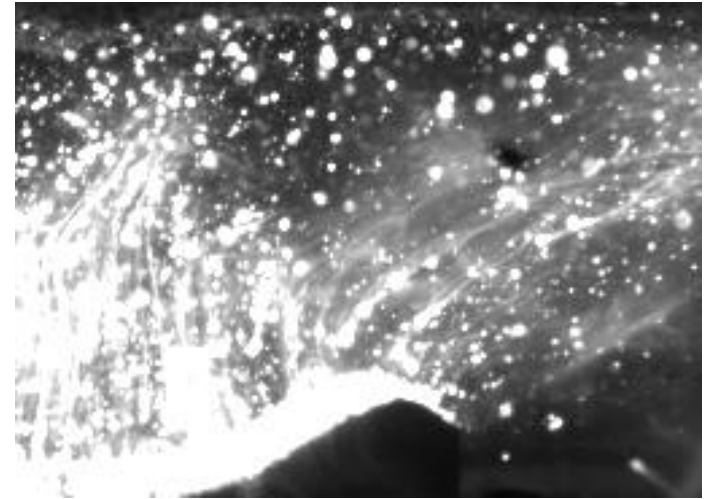
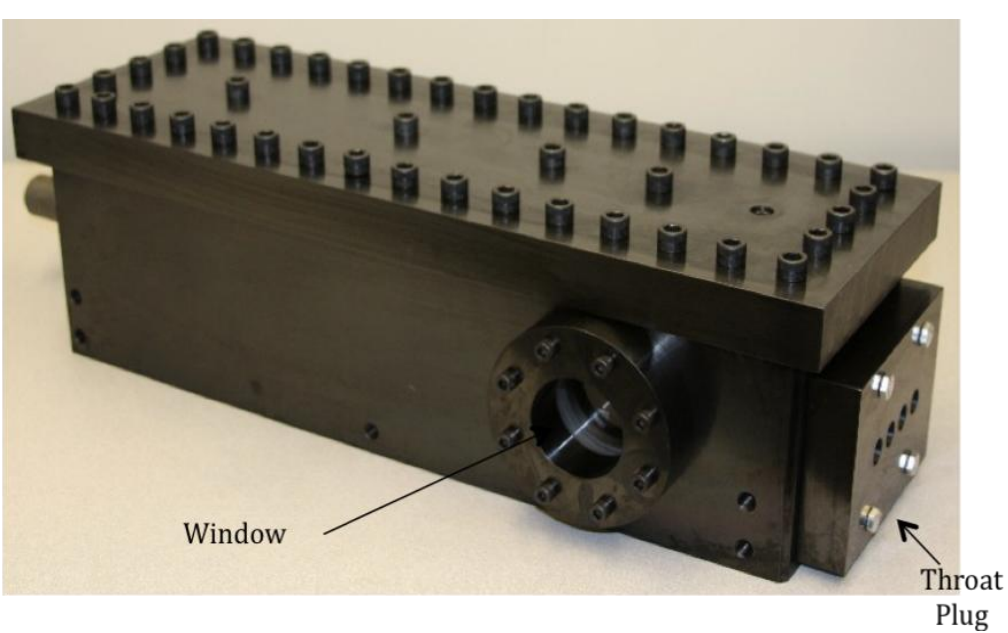
Particle Diameter for PBAN/AP/AI Propellant at 1 atm



- Particle Size can be approximated with a normal distribution
- Average Diameter of .011 in. (281  $\mu\text{m}$ )
- 95% Confidence for Calculations

Distribution A: Approved for public release;  
distribution unlimited

# AGGLOMERATION IN CROSS FLOW



- Windowed combustor currently in use for erosive burning experiments
- Pressurized with argon gas to simulate cross flow
- No clear imaging of particle coalescence and fragmentation as of yet
- System feasibility has been demonstrated

Distribution A: Approved for public release;  
distribution unlimited

# FUTURE WORK

- Redesign of windowed combustor
- Further velocimeter development and validation
- Velocity mapping inside the solid rocket motor (SRM)
- Particulate Characterization inside of SRM
- Temperature Concentrations inside of SRM using spectroscopy
- Formulation of different propellant combinations based on binder
- Effects of agglomeration by addition of intermetallics (ex. Al-Ni)

# ACKNOWLEDGMENTS

- Research Sponsored by the Department of Airforce SBIR contract No. FA9300-08-M-3022
- Special Thanks to Hieu Nguyen at the Air Force Research Lab for his advice and encouragement
- Thanks to all the graduate students and support staff at the Purdue University Energetic Materials Lab for their help and guidance

# REFERENCES

1. Cheung, H., Cohen, N. S., "Performance of Solid Propellants containing metal Additives," *AIAA Journal* 3(2), 250-257 (1964).
2. Price, E. W., "Combustion of Metalized Propellants," Chap. 9 in *Fundamentals of Solid-Propellant Combustion*, Kuo, K. K. and Summerfield, M (eds.), American Institute of Aeronautics and Astronautics, Inc., New York, pp 479-513 (1984).
3. Sambamurthi, J. K., Price, E.W., and Sigman, R. K., "Aluminum Agglomeration in Solid-Propellant Combustion," *AIAA Journal* 22(8), 1132-1138 (1984).
4. Hermsen, R. W., "Aluminum Oxide Particle Size for Solid Rocket Motor Performance Prediction, Proc. AIAA 19<sup>th</sup> Aerospace Sciences Meeting, Louis Missouri (January 1981).
5. Laredo, D., McCrorie, J. D., Vaughn, J. K., Netzer, D. W., "Motor and Plume Particle Size Measurements in Solid Propellant Micromotors," *Journal of Propulsion and Power* 10(3), 410-418 (1994).
6. Kovalev, O. B., "Motor and Plume Particle Size Prediction in Solid-Propellant Rocket Motors," *Journal of Propulsion and Power* 18(6), 1199-1210 (2002).

Distribution A: Approved for public release;  
distribution unlimited

# REFERENCES (CONT.)

7. Melcher, J. C., Burton, R. L., Krier, H., "Combustion of Aluminum Particles in Solid Rocket Motor Flows," Proc. 35<sup>th</sup> AIAA/ASME/SAE/ASEE Joint Propulsion Conference and Exhibit, Los Angeles, CA (June 1999).
8. Mullen, J. C., Brewster, M. Q., "Characterization of Aluminum at the Surface of Fine-AP/HTPB Composite Propellants," Proc. 44<sup>th</sup> AIAA/ASME/SAE/ASEE Joint Propulsion Conference and Exhibit, Hartford, CT (July 2008).
9. Averin, V. S. , Arkhipov, V. A., Vasenin, I. M., Dyachenko, N. N., Trofimov, V. F., "Effect of a Sudden Change in Cross-Sectional Area of the Solid Rocket Motor Duct on Coagulation of Condensed Particles," *Combustion, Explosion and Shock Waves* 39(3), 316-322 (2003).
10. Jackson, T. L., Najjar, F., Buckmaster, J., "New Aluminum Agglomeration Models and Their Use in Solid-Propellant Rocket Simulations," *Journal of Propulsion and Power* 21(5), 926-936 (2005).
11. Cohen, N. S., "A Pocket Model for Aluminum Agglomeration in Composite Propellants," Proc. 17<sup>th</sup> AIAA/SAE/ASME Joint Propulsion Conference, Colorado Spring, CO (July 1981).

Distribution A: Approved for public release;  
distribution unlimited

# Experimental Characterization of Particle Dynamics within Solid Rocket Motors

By  
Joseph Moore  
&  
Steve F. Son, Ph.D.  
Purdue University

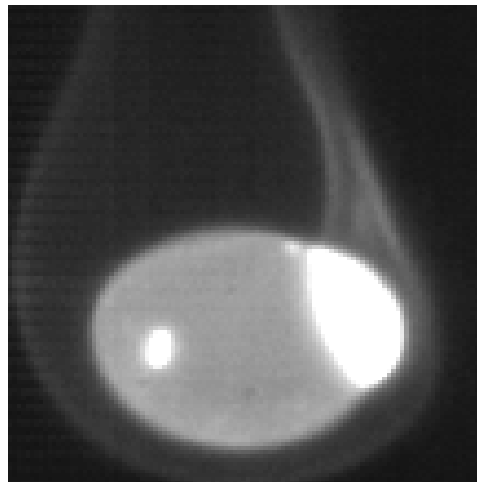
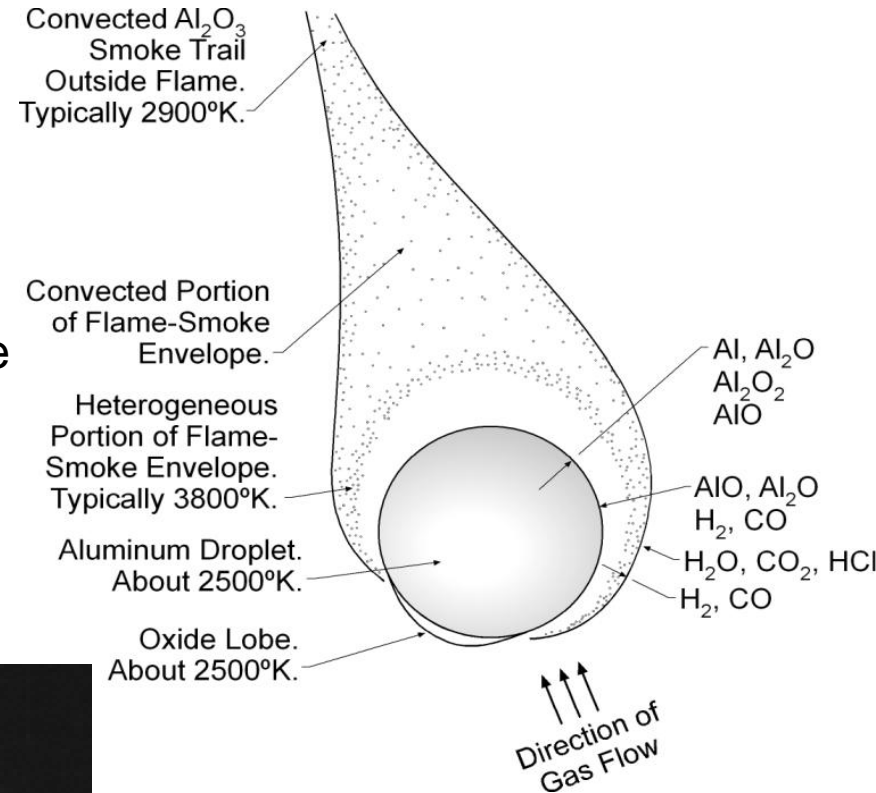
Yudaya Sivanathu, Ph.D.  
&  
Jongmook Lim, Ph.D.  
En'Urga Laboratories

Distribution A: Approved for public release; distribution unlimited

This research is sponsored by the Department of Air Force AFFTC/PKTB under the Small Business Innovative Research contract No. FA9300-08-M-3022.

# UNDERSTANDING OF THE PROBLEM

- Advantages to Aluminized propellants
  - Increase in specific impulse
  - Can suppress combustion instabilities
- Incomplete combustion of Al
  - Unfavorable ignition conditions on surface
  - Agglomerate into larger particles
  - Efficiency losses in system leads to decreased Isp from ideal



# PREVIOUS RESEARCH

- Price
  - Aluminum droplet model
  - Chain agglomeration for HTPB/AP/Al propellant
- Cohen
  - “Pocket Model”
  - Bi-modal AP distribution
  - Agglomeration between large particles
- Sambamurthi
  - Expanded on Pocket Model
  - Found that unfavorable ignition conditions in pockets led to large agglomerates
  - Certain conditions lead to the formation of “superagglomerates”
- Hermsen
  - Particle size v. throat diameter
- Averin
  - Effect of sudden changes in area
  - Size increase by factor of 8 from initial measurements

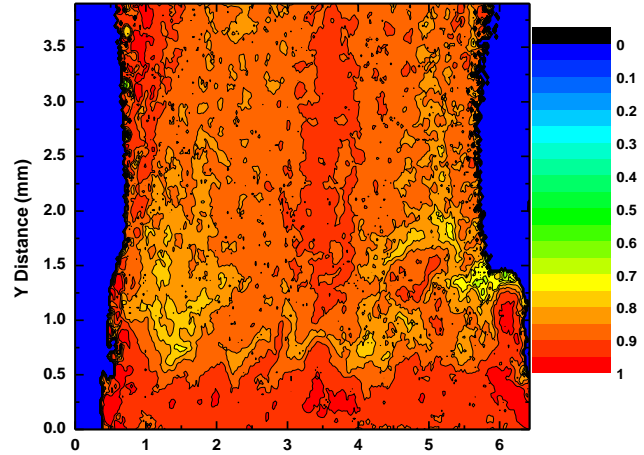
# PREVIOUS RESEARCH (CONT.)

- Kovalev
  - Agglomeration size v. composition, P, rb, AP size distribution
  - Based on experimental results
  
- Melcher
  - Digital background subtraction/high-pass filter
  - 16.4 ft/s (5 m/s) agglomeration size at 13 atm
  
- Mullen
  - Agglomerate size v. fine AP loading
  - 0.008 in. (200 micron) agglomerates at 3 atm
  
- Averin
  - Particle size based on sudden change (both increase and decrease) in motor area
  - Focused on both coagulation and fragmentation of particles

# OBJECTIVES

- Develop a statistical correlation velocimeter for obtaining high speed videos within a solid rocket motor
- Develop a high resolution imaging system to directly image particulates near the burn surface of a solid propellant inside a rocket motor
- Evaluate the two systems using a segment solid rocket motor

# STATISTICAL IMAGE CORRELATION VELOCIMETRY



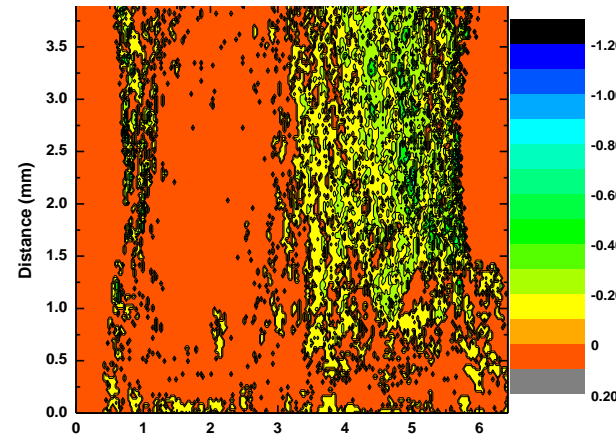
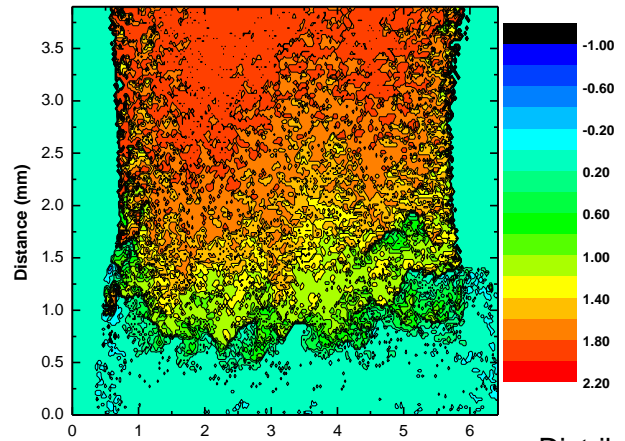
$$S_{ij} = \frac{\sum_{k=1}^N \left| \overline{V_k^i(t) - V^i(t)} \right| * \left| \overline{V_k^j(t') - V^j(t')} \right|}{N \sqrt{\sigma_i(t) \cdot \sigma_j(t')}}$$

•Inputs:

- High speed images
- Scale

•Outputs:

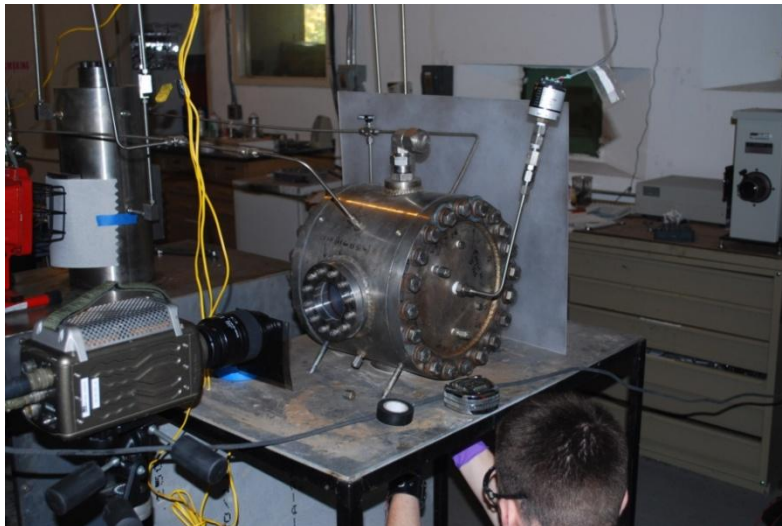
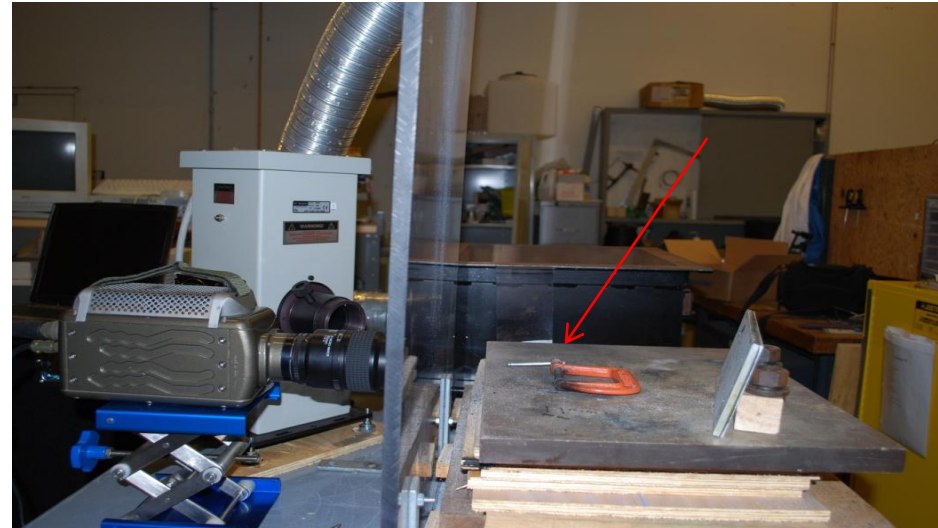
- Axial velocity
- Radial velocity
- Correlation coefficient



Distribution A: Approved for public release;  
 distribution unlimited

# IMAGING SYSTEM

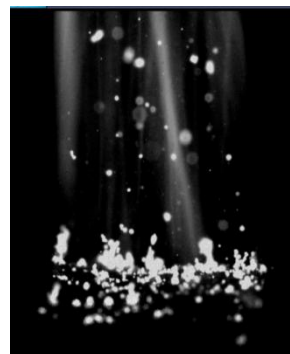
- Phantom High Speed Camera
  - 6000 fps
  - 512x512 resolution
  - Later decreased to 256x256
  - 1-3  $\mu$ s exposure time
- 1000W Xenon Lamp
- ~5 second burn time



- 4 atm testing inside of pressure vessel
- Argon gas used for pressurization

Distribution A: Approved for public release;  
distribution unlimited

# AGGLOMERATION BASED ON BINDER



## HTPB/AP/Al propellants

- Flakes of Aluminum agglomerate into small particles which chain together before detaching from the burning surface

•Time between images: 167  $\mu$ s

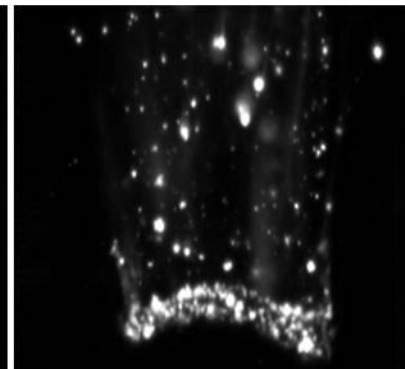
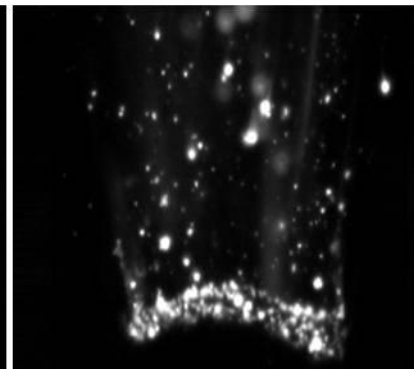
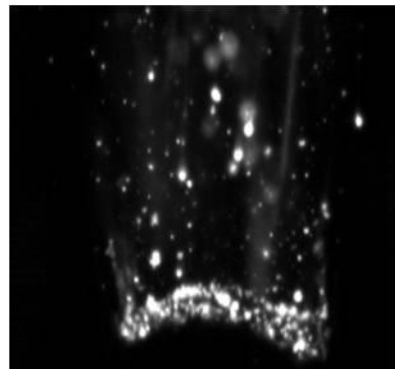
## PBAN/AP/Al Propellant

- Flakes of aluminum agglomerate downward toward surface into spherical particles

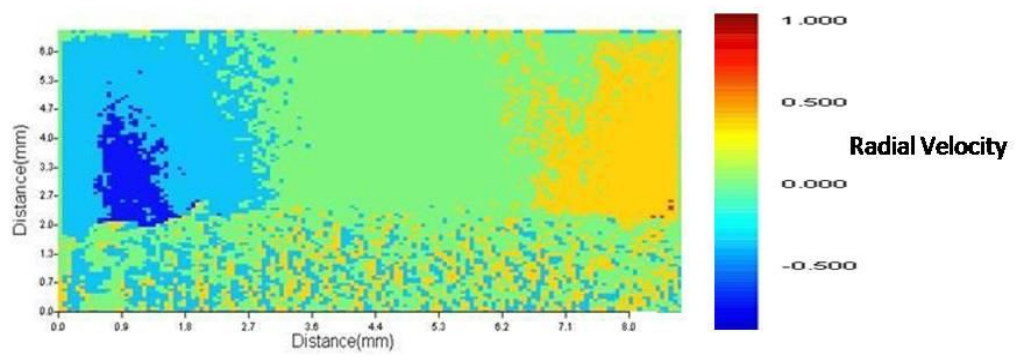
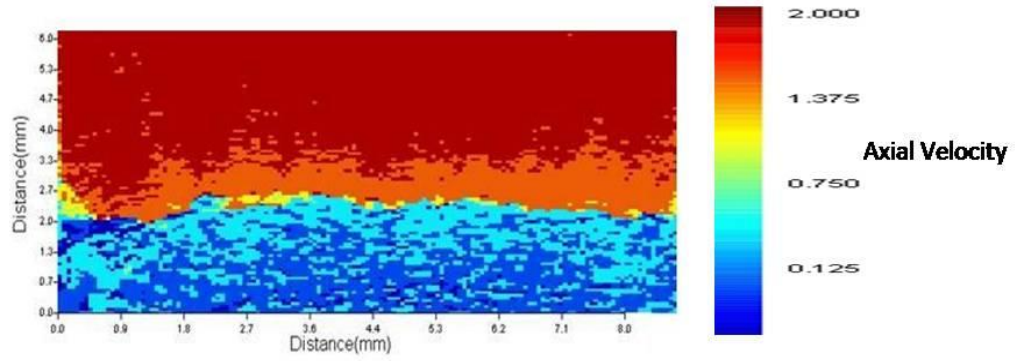
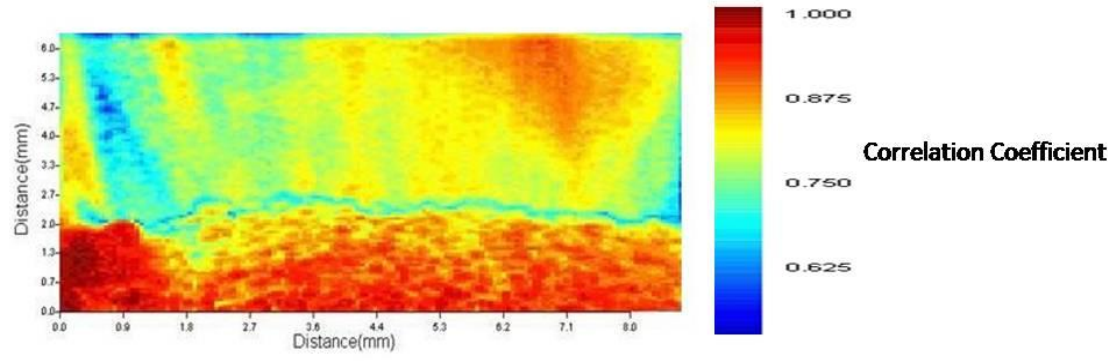
•Time between images:

167  $\mu$ s

Distribution A: Approved for public release; distribution unlimited



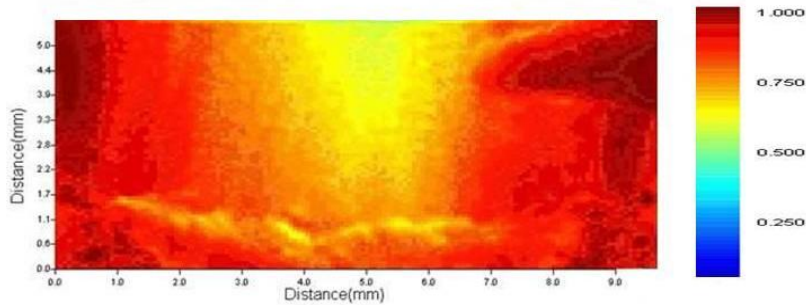
# PBAN/AP/AL AT 1 ATM



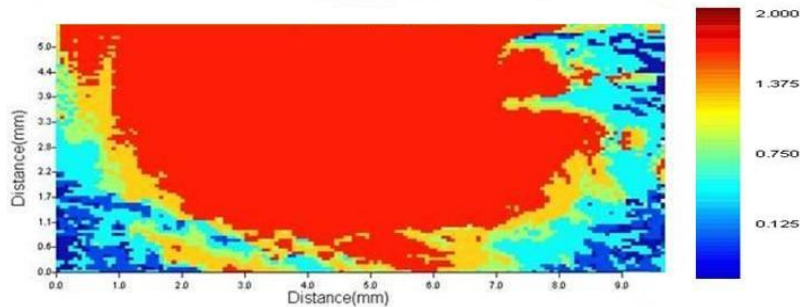
- High values for correlation coefficient
- Maximum velocity of  $\sim 6.33$  ft/s (1.93 m/s)
- Recirculation zones near edges of propellant due to clamping device

Distribution A: Approved for public release; distribution unlimited

# PBAN/AP/AL PROPELLANT AT 4 ATM

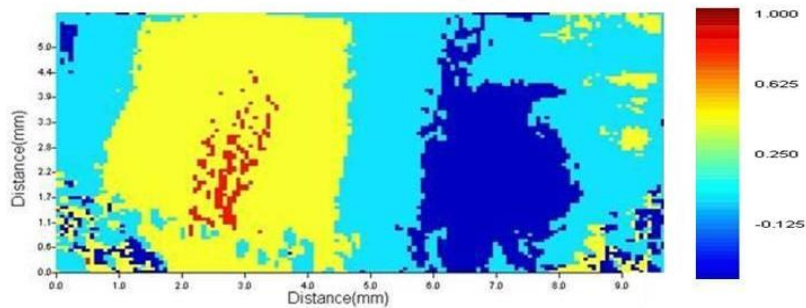


- High values for correlation coefficient



- Decreased maximum velocity  
~5.38 ft/s (1.64 m/s)

- Decrease in velocity validated by a discussion of continuity



Distribution A: Approved for public release;  
distribution unlimited

# DISCUSSION OF CONTINUITY

- Mass continuity for control volume is

$$\rho_c r_b A = \rho_g VA$$

- Burning rate (St. Roberts Law)

$$r_b = aP_c^n$$

- Ideal gas equation

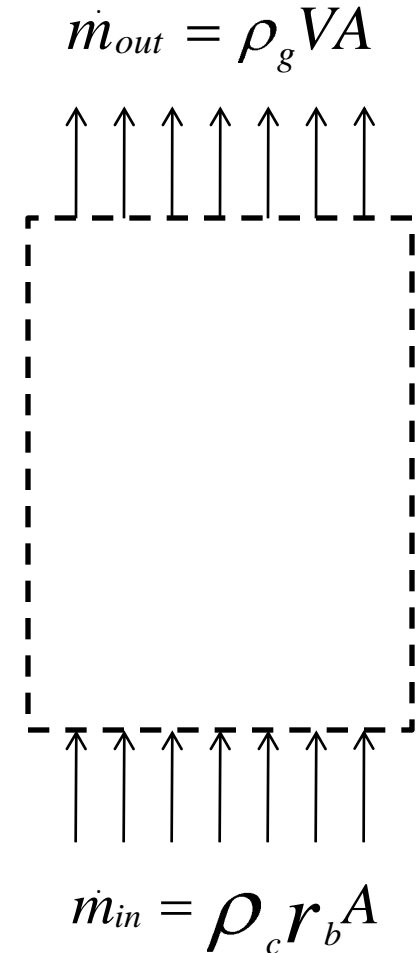
$$\rho_g = \frac{P_g}{RT_g}$$

- Combining to get velocity dependency

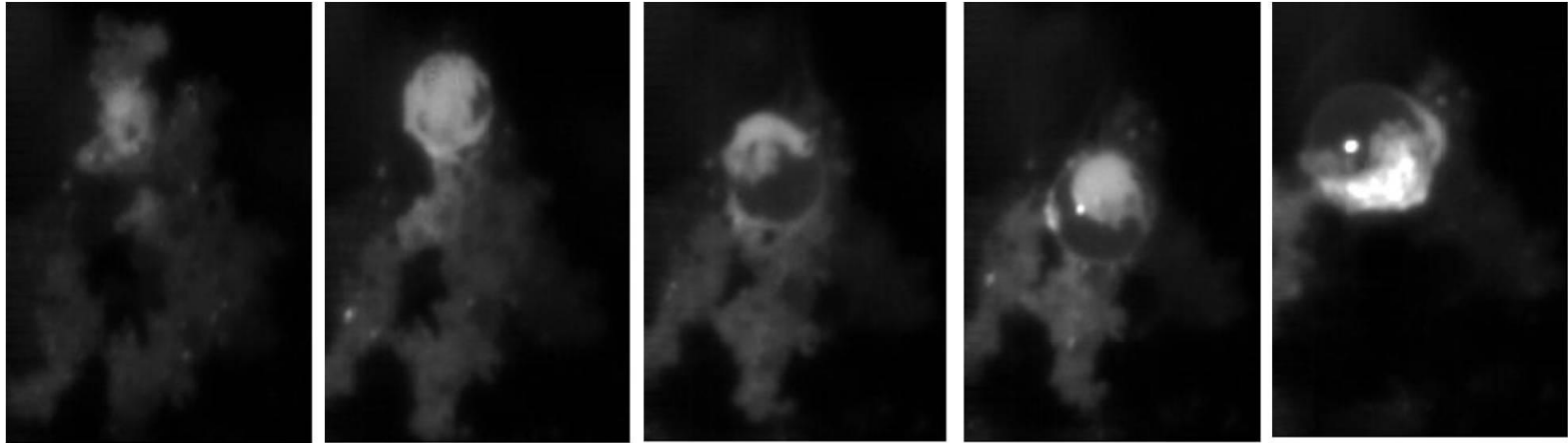
$$V = CP_g^{n-1}$$

$$C = a\rho_c RT_g$$

- Velocity is inversely proportional to Pressure



# MICROSCOPIC IMAGING

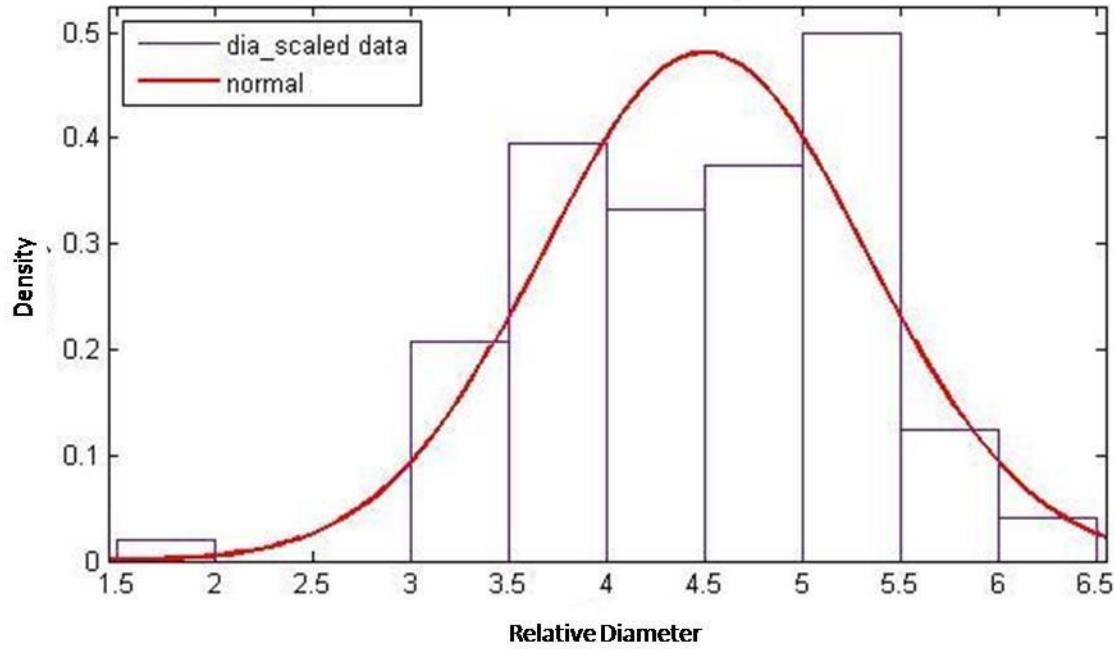


- PBAN/AP/Al Agglomerate at 1 atm
- Surface Tension drives particle toward burning surface until it is overcome by Aerodynamic forces
- Time  $\sim 2.4$  ms for above sequence
- Images analysis can be automated for particle sizing

Distribution A: Approved for public release;  
distribution unlimited

# PARTICLE SIZING

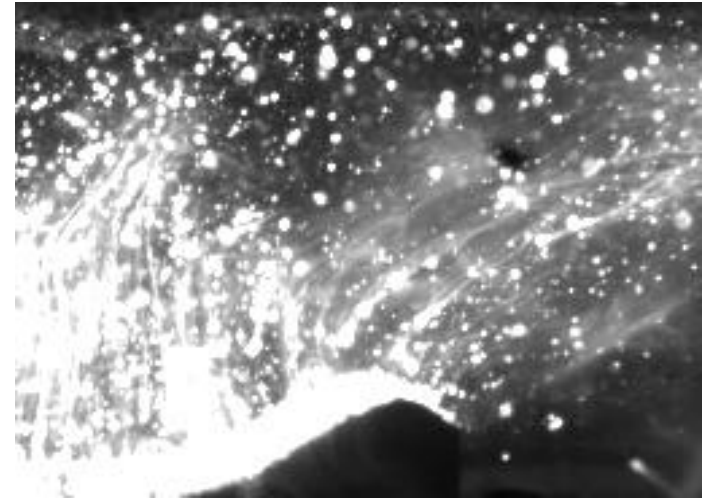
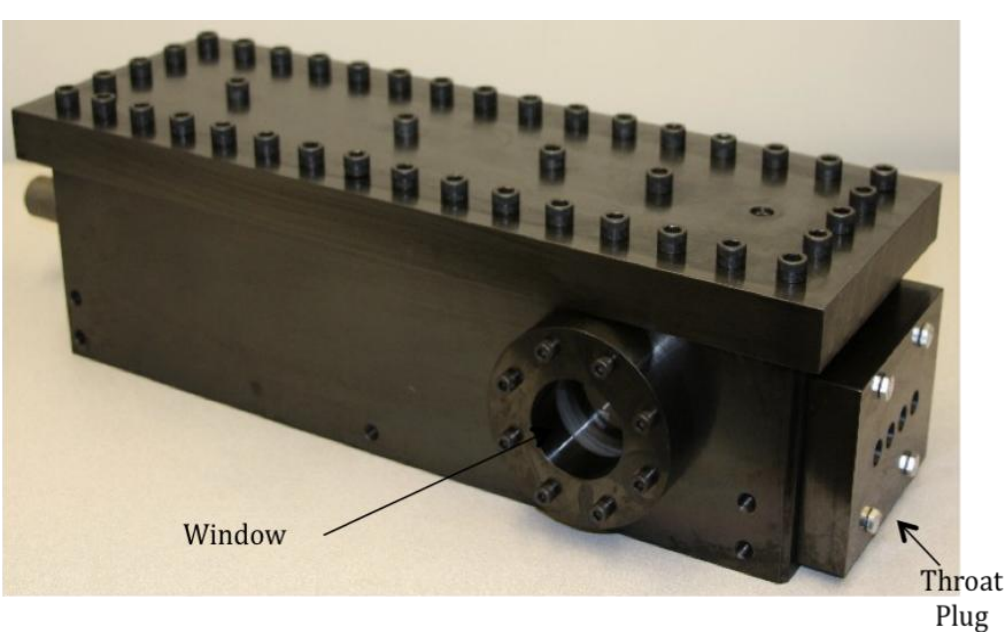
Particle Diameter for PBAN/AP/AI Propellant at 1 atm



- Particle Size can be approximated with a normal distribution
- Average Diameter of .011 in. (281  $\mu\text{m}$ )
- 95% Confidence for Calculations

Distribution A: Approved for public release;  
distribution unlimited

# AGGLOMERATION IN CROSS FLOW



- Windowed combustor currently in use for erosive burning experiments
- Pressurized with argon gas to simulate cross flow
- No clear imaging of particle coalescence and fragmentation as of yet
- System feasibility has been demonstrated

Distribution A: Approved for public release;  
distribution unlimited

# FUTURE WORK

- Redesign of windowed combustor
- Further velocimeter development and validation
- Velocity mapping inside the solid rocket motor (SRM)
- Particulate Characterization inside of SRM
- Temperature Concentrations inside of SRM using spectroscopy
- Formulation of different propellant combinations based on binder
- Effects of agglomeration by addition of intermetallics (ex. Al-Ni)

# ACKNOWLEDGMENTS

- Research Sponsored by the Department of Airforce SBIR contract No. FA9300-08-M-3022
- Special Thanks to Hieu Nguyen at the Air Force Research Lab for his advice and encouragement
- Thanks to all the graduate students and support staff at the Purdue University Energetic Materials Lab for their help and guidance

# REFERENCES

1. Cheung, H., Cohen, N. S., "Performance of Solid Propellants containing metal Additives," *AIAA Journal* 3(2), 250-257 (1964).
2. Price, E. W., "Combustion of Metalized Propellants," Chap. 9 in *Fundamentals of Solid-Propellant Combustion*, Kuo, K. K. and Summerfield, M (eds.), American Institute of Aeronautics and Astronautics, Inc., New York, pp 479-513 (1984).
3. Sambamurthi, J. K., Price, E.W., and Sigman, R. K., "Aluminum Agglomeration in Solid-Propellant Combustion," *AIAA Journal* 22(8), 1132-1138 (1984).
4. Hermsen, R. W., "Aluminum Oxide Particle Size for Solid Rocket Motor Performance Prediction, Proc. AIAA 19<sup>th</sup> Aerospace Sciences Meeting, Louis Missouri (January 1981).
5. Laredo, D., McCrorie, J. D., Vaughn, J. K., Netzer, D. W., "Motor and Plume Particle Size Measurements in Solid Propellant Micromotors," *Journal of Propulsion and Power* 10(3), 410-418 (1994).
6. Kovalev, O. B., "Motor and Plume Particle Size Prediction in Solid-Propellant Rocket Motors," *Journal of Propulsion and Power* 18(6), 1199-1210 (2002).

Distribution A: Approved for public release;  
distribution unlimited

# REFERENCES (CONT.)

7. Melcher, J. C., Burton, R. L., Krier, H., "Combustion of Aluminum Particles in Solid Rocket Motor Flows," Proc. 35<sup>th</sup> AIAA/ASME/SAE/ASEE Joint Propulsion Conference and Exhibit, Los Angeles, CA (June 1999).
8. Mullen, J. C., Brewster, M. Q., "Characterization of Aluminum at the Surface of Fine-AP/HTPB Composite Propellants," Proc. 44<sup>th</sup> AIAA/ASME/SAE/ASEE Joint Propulsion Conference and Exhibit, Hartford, CT (July 2008).
9. Averin, V. S. , Arkhipov, V. A., Vasenin, I. M., Dyachenko, N. N., Trofimov, V. F., "Effect of a Sudden Change in Cross-Sectional Area of the Solid Rocket Motor Duct on Coagulation of Condensed Particles," *Combustion, Explosion and Shock Waves* 39(3), 316-322 (2003).
10. Jackson, T. L., Najjar, F., Buckmaster, J., "New Aluminum Agglomeration Models and Their Use in Solid-Propellant Rocket Simulations," *Journal of Propulsion and Power* 21(5), 926-936 (2005).
11. Cohen, N. S., "A Pocket Model for Aluminum Agglomeration in Composite Propellants," Proc. 17<sup>th</sup> AIAA/SAE/ASME Joint Propulsion Conference, Colorado Spring, CO (July 1981).

Distribution A: Approved for public release;  
distribution unlimited